63 3-3

402668

FINAL TECHNICAL REPORT ON THE NUCLEAR PROPERTIES OF RHENIUM

402 668

for

Department of the Navy
Bureau of Weapons
Washington 25, D. C.

under

Contract No.: NOas 60-6021-c

by: R. A. Karam
T. F. Parkinson
W. H. Ellis

Department of Nuclear Engineering
University of Florida
Gainesville, Florida

FOR ERRATA

AD 402668

THE FOLLOWING PAGES ARE CHANGES

TO BASIC DOCUMENT

ERRATA

FINAL TECHNICAL REPORT

ON

THE NUCLEAR PROPERTIES OF RHENIUM

FOR

DEPARTMENT OF THE NAVY
BUREAU OF WEAPONS
WASHINGTON 25, D. C.

under

CONTRACT NO.: NOas 60-6021-c

December, 1963

Written by: R. A. Karam
T. F. Parkinson
W. H. Ellis

Department of Nuclear Engineering
University of Florida
Gainesville, Florida

ERRATA

Decay Scheme of Re^{184} and Re^{184m}*

The decay scheme shown in Figure 16 was calculated using the collective model of the nucleus. On the basis of this model, level assignments were made as shown in Table X to account satisfactorily for all the observed transitions. However, the assignment of a spin-parity of $(0, 8^{+})$ to the 1240 keV level appears to be extremely unlikely, since the transition from the 3- ground state of Re-184 to such a level is a fifth-forbidden one [1]. Accordingly the spin-parity assignment for this level should be regarded as unknown.

In addition, the beta vibrational band should have K and I values of 0 rather than 2 as shown in Fig. 16 [1].

---

* See Appendix B of Final Technical Report on the Nuclear Properties of Rhenium, Department of the Navy, Bureau of Weapons, Washington 25, D. C., R. A. Karam, *et al.*, March 1, 1963.

[1] Private Communication from C. Sharp Cook.

FINAL TECHNICAL
REPORT

ON

THE NUCLEAR PROPERTIES OF RHENIUM

FOR

DEPARTMENT OF THE NAVY
BUREAU OF WEAPONS
WASHINGTON 25, D. C.

under

CONTRACT NO.: NOas 60-6021-c

March 1, 1963

Written by: R. A. Karam
T. F. Parkinson
W. H. Ellis

Department of Nuclear Engineering
University of Florida
Gainesville, Florida

Final Technical Report,
Contract NOas 60-6021-c

LIST OF CONTRIBUTORS

C. A. Bisselle

W. H. Ellis

R. A. Karam

E. E. Menge

F. J. Munno

T. F. Parkinson

John A. Wethington, Jr.

Final Technical Report,
Contract NOas 60-6021-c

TABLE OF CONTENTS

LIST OF TABLES

LIST OF FIGURES

Final Technical Report,
Contract NOas 60-6021-c

ABSTRACT

The thermal neutron activation cross sections of Re^{185} and Re^{187} were measured and found to be 96.5 $\pm$ 10 barns and 88 $\pm$ 14 barns, respectively. The effective resonance integral of natural rhenium was measured to be 694 $\pm$ 28 barns including the $\frac{1}{v}$ component.

The (n, 2n) cross sections of Re^{185}, Re^{187} and Re^{185} (n,2n)Re^{184m} with 14.1 Mev neutrons were measured and found to be 1.91 $\pm$ 0.6 barns, 1.44 $\pm$ 0.41 barns and 1.12 $\pm$ 0.4 barns, respectively. The (n, α) reaction with 14.1 Mev neutrons was investigated theoretically and it was concluded that this reaction does not occur. The (n,p) reaction was also investigated on a theoretical basis and it was found that this reaction is improbable with 14.1 Mev neutrons. The cross section of this reaction was calculated to be 32.2 millibarns. This calculation however, could be in error by a factor of 10.

The capture gamma rays reported here are the work of Groshev, et.al. (12)

The decay scheme of Re^{184} - Re^{184m} is proposed and the gamma rays from Au^{196} and Au^{196m} were studied.

---

^{m} Indicate metastable state of Re^{184} and Au^{196}

Comparison of the shielding properties of rhenium and lead for thermal neutrons was made on a theoretical basis. A technique for separating gamma ray pulses from neutron pulses in NaI (Tl) detectors is also included.

INTRODUCTION

The high density, high melting point, and the relatively high thermal and resonance neutron cross sections of rhenium metal make it an attractive material for use in shielding and control applications. However, prior to such applications, one must know the nuclear, chemical and the metallurgical properties of that material. Sims et. al.(1) conducted a comprehensive survey of the published literature covering all work reported on the element up to 1956. Their survey covered the chemical, metallurgical, electrical and nuclear properties of the metal. This final report covers those nuclear properties of rhenium that have been studied at the University of Florida.

The possible uses of rhenium in a nuclear reactor are (1) shielding material and (2) control rod material. The high density of rhenium (20.53 gm/cm^3) offers a substantial saving in the weight of a mobile reactor shield.(2) The relatively high thermal cross section, the high effective resonance integral and the high melting point of rhenium make it an attractive control rod material for power reactors.

ACTIVATION CROSS SECTIONS BY THERMAL NEUTRONS

The activation cross sections of Re^{185} and Re^{187} were

measured relative to gold. A 7/16 in. diameter by 0.005 in. thick gold disk and a small gold wire were placed 24 in. apart along the central axis of the University of Florida Training Reactor (UFTR) thermal column and irradiated. The small gold wire was used as a flux monitor. The activity of the wire was counted integrally and the activity of the disk was analyzed differentially by a multi-channel analyzer with a 1 3/4 in.diameter by 2 in. thick NaI (Tl) crystal. The same experiment was repeated using a natural rhenium disk with the same dimensions as the gold disk and a gold wire.

The activation cross section for Re^{185} was computed from the relationship

$$\sigma_{Re^{185}} = \frac{I_2^o \, e_1 f_1 \phi_1 M_1 A_2 (1-e^{-\lambda_1 t_1}) \, \sigma_1}{I_1^o \, e_2 f_2 \phi_2 M_2 A_1 (1-e^{-\lambda_2 t_2})} \tag{1}$$

where the subscripts 1 and 2 refer to gold and rhenium respectively. The other symbols are

I^o = the counting rate of a particular gamma quantum from the disk at the time of reactor shutdown,

e = efficiency of the crystal as a function of energy and geometry

f = fraction of unconverted photon quanta of a particular energy per disintegration of the nuclide in question

ϕ_1 = neutron flux computed from the specific activity of the gold wire irradiated with the gold disk,

ϕ_2 = neutron flux computed from the specific activity of the gold wire irradiated with the rhenium disk,

M = mass of a particular isotope in a disk,

A = atomic mass of the particular isotope,

λ = decay constant for the particular isotope,

t = time of irradiation, and

σ = activation cross section.

The activation cross section for Re^{187} was computed from a similar equation.

In determining the activation cross sections, the rhenium disk and the gold disk counting rates were considered as the sum of the pulses in all channels from 36 through 179. By considering only these channels, X-ray production in either the crystal or the samples was eliminated, and only the photo-peaks and Compton peaks were counted. The rhenium disk was counted for a total of 250 hours. The activity of the sample after 160 hours of decay was mainly Re^{186}. The fifty counting rates obtained for this isotope were collected into ten groups of five experimental results. The average counting rate of each group was determined by the techniques given in Overman and Clark.(3) The half-life of the isotope was obtained by

averaging the values tabulated by Strominger, Hollander, and Seaborg,[4] and this value was used to extrapolate each group back to the time of neutron irradiation termination. These ten initial counting rates were averaged to give I_2^o in Equation 1. The counting rate of Re^{186} at any time was then computed from I_2^o. The contribution of Re^{186} was subtracted from the gross counting rates to give the counting rate of Re^{188} at any experimental point in the time interval 20-160 hr.

These data were then treated in exactly the same manner to determine the initial counting rate of the Re^{188} in the sample. The data from the gold disk were treated in the same way to give I_1^o. No subtraction was necessary since gold is a monoisotopic element.

Counting rates for each Re isotope and for Au were converted into absolute activities by the procedure of Vegors, Marsden, and Heath.[5] This conversion is represented by e in Equation 1.

The value of f_2 used to calculate the activation cross section for Re^{185} was taken from the work of Jones, McMullen, Williams, and Nablo[6] and from the work of Macklin, Lazar, and Lyon.[7] The value of f_1 for gold was 0.961 as derived

from the data in Strominger et.al.[4] The decay constants were obtained by averaging the values listed in the same table.

Results

Half-lives.-- Rhenium^{186} was found to have a half-life of 89 hr. The half-life of the isomeric transition in Re^{188} was found to be 19 min., and the half-life for the beta decay of this isotope, measured by gamma counting, was 17 hr.

Identification of Peaks.-- Figure 1 shows the pulse height spectra of an activated sample of rhenium shortly after removal from the reactor. The first peak on the left is caused by iodine X rays. The second peak results from osmium X rays, 60.96 Kev., and the 64 Kev. gamma quanta from the isomeric transition of Re^{188}. The hump at the base of the third peak is caused by the 92 Kev. isomeric transition of Re^{188} plus coincident photons normally registered in the first two peaks. The third peak is caused by the 105 Kev. gamma quanta from the isomeric transition of Re^{188}. The hump on the left side of the fourth peak is caused by the 122 Kev. gammas emitted from W^{186} following the decay of Re^{186} by electron capture and by the 137 Kev. gamma rays from Os^{186} following the decay of Re^{186} by beta emission. The fourth peak, according to these measurements, is caused by the 152 Kev. gamma photons

emitted by Os^{188} resulting from the beta decay of Re^{188}. The energy of this gamma photon has been reported as 155 Kev., but the data in Figure 1 indicate a value of 152 Kev. The instrument was quite linear and consequently, this difference is not caused by non-linear response. The presence of other photons may cause this discrepancy. Irradiation of pure Re^{187} would verify this point. The hump on the right of the fourth peak is caused by coincidence of two or more scattered or primary photons. Some higher energy photons such as 478 Kev. and 633 Kev. quanta from Re^{188} were identified, but these are not included in Figure 1.

Figure 2 shows the pulse height spectra of the sample 54 hr. after the irradiation. The 105 and 92 Kev. peaks are almost depleted, but they are still resolved. The 137 and 152 Kev. peaks are more distinct than in Figure 1 because the reduction in intensity permitted better resolution.

Activation Cross Section, Re^{185}.-- In determining the value of the activation cross section of Re^{185}, the value of f_2 as defined in Equation 1 was taken to be 0.111. This value is the sum of the fractions of the 137 Kev. and the 122 Kev. gamma rays per Re^{186} nucleus undergoing disintegration. These

fractions[(4), (5)] were 0.105 and 0.006 respectively.

The activation cross section computed for Re^{185} was 96.5 $\pm$ 10 barns. The standard deviation assigned to this result was computed by using the equations given in Overman and Clark.[(8)]

Activation Cross Section, Re^{187}.-- The value of f_2 reported by Jones et.al.[(6)] was 0.09 while the value reported by Macklin et.al.[(7)] was 0.169. These two values of f_2 led to activation cross sections of 187 $\pm$ 22 barns and 104 $\pm$ 17 barns respectively. A value for f_2 as calculated from the percentage of Os^{188} de-exciting through the 155 Kev. level (21.4%)[(9)] per decay and the internal conversion coefficient given by M. E. Rose[(10)] for E_1 transition, is 0.20. With this value for f_2, the activation cross section for Re^{187} was found to be 88 $\pm$ 14 barns. This last value for the activation cross section of Re^{187} is in agreement with values measured by other workers as shown in Table I.

TABLE I

COMPARISON OF ACTIVATION CROSS SECTION, σ ACTIVATION, WITH OTHER WORKERS

Source	$\sigma_{act.}$ Re^{185}	$\sigma_{act.}$ Re^{187}	Half-life Re^{186}	Half-life Re^{188m}	Half-life Re^{188}
This work	96.5 ± 10	88 ± 14	89 hrs	19 min	17 hrs
Seren *et.al.*[11]	101 ± 20	75.3 ± 15	90 hrs	-	18 hrs
Groshev *et.al.*[12]	100 ± 8	63 ± 5	91 hrs	-	16.7 hrs
Pomerance [13]	100 ± 8	-	-	-	-

The activation cross sections for Re^{185} and Re^{187} reported here are in good agreement with the results reported by other workers as shown in Table I. Spectra from the decay of Re^{186} and Re^{188} agree generally with the decay schemes given in the Nuclear Data Sheets[9] and the "Table of Isotopes."[4] In addition, the spectra showed three quanta associated with the isomeric transition of Re^{188}. The energies of these gamma rays are 105, 92 and 64 Kev. and all have a half-life of 19 minutes. This observation is in agreement with the finding of V. S. Dzelepov and L. K. Peker.[14]

EFFECTIVE RESONANCE INTEGRAL

It has been customary in determining the activation resonance integral, RI, of a sample to measure the cadmium ratios of the sample and a standard and then to employ the

following relationship

$$(RI)_x = (RI)_s \frac{\left[Q(t) \quad \left(\frac{CdR(t)}{F} - 1\right)\right]_s}{\left[Q(t) \quad \left(\frac{CdR(t)}{F} - 1\right)\right]_x} \quad \frac{(\sigma\ th)x}{(\sigma\ th)s} \tag{2}$$

to get the activation resonance integral of the sample.[15]

In Equation (2), the subscripts s and x refer to the standard and the sample. The other symbols are defined as follows:

CdR = the cadmium ratio,

Q(t) = self shielding correction factor for a foil of thickness t, (approaches 1 as $t \longrightarrow 0$)

F = a correction factor to account for the epithermal neutron absorption by the cadmium, and

σ_{th} = thermal neutron activation cross section.

In Equation (2) it is assumed that the cross sections of the sample and the standard have identical energy dependence in the sub-cadmium region. The F factor can be readily calculated if one assumes an incident isotropic flux of epithermal neutrons. With this assumption the ratio of the outgoing to the incoming epithermal flux is[16]

$$\frac{\phi_1}{\phi_o} = \frac{\int_o^1 e^{-\Sigma_a t/\mu} \, d\mu}{\int_o^1 d\mu} \tag{3}$$

where ϕ_1 = the epithermal flux after traversing the cadmium cover,

ϕ_o = the incident epithermal flux,

Σ_a = the macroscopic absorption cross section of cadmium at the resonance energy of the foil,

$\mu = \cos\theta$.

Integration of Equation (3) yields

$$\frac{\phi_1}{\phi_o} = E_2(\Sigma_a t) \tag{4}$$

and $F = 1/E_2(\Sigma_a t)$. (5)

Experimental.-- The cadmium ratios of gold, indium, and rhenium were measured as a function of foil thickness. The thinnest foil of each material was prepared by evaporation on a thin backing ($1 mg/cm^2$) of aluminum. Each of the aluminum backings was weighed on a Cahn electrobalance four times and the average was taken. The weighing procedure was repeated after the films were deposited. Particular care was taken to keep these foils clean and dry.

The aluminum alone was activated and its decay was studied with time. The bare aluminum foils were irradiated at a certain power level in the center of the University of Florida Training Reactor. The cadmium covered foils were irradiated at the same

position and the same power level. Gold wire detectors were used to normalize the Cd covered and bare activations. The same procedure was repeated for the Au, In, and Re foils. The cadmium covers in all cases were 0.035 in. thick. The cadmium covers consisted of two flat sheets, one larger than the other. The overlapping parts of the larger sheet were bent around the smaller sheet. Gamma-ray scintillation counting with a NaI (Tl) well-type crystal was employed for all cases.

Results

Figures 3, 4 and 5 show the cadmium ratio versus foil thickness for Au, In, and Re, respectively. Gold was used as a standard and indium was used as a secondary standard to check on the experimental procedure. The correction factors for the absorption of epithermal neutrons in the cadmium cover, as calculated from Equation (5) were 1.03, 1.06 and 1.04 for gold, indium, and rhenium. In calculating these values, the total macroscopic cross section of cadmium was used at the various resonance energies instead of the absorption cross section. Thus, any scattering of resonance neutrons that may remove these neutrons from the vicinity of the foils is taken into account.

Equation (2) was used to calculate the activation resonance integral. The values of Q(t) were taken to be unity for the thin films. Table II summarizes the results.

TABLE II

RESONANCE ACTIVATION INTEGRALS**

Material	σ_{act}(2200m/sec) Barns	Thickness cm	Experimental Value, RI Barns	Literature Value, Barn	Ref.
Au^{197}	96 $\pm$ 10	8.34×10^{-6}	1558(Ref)	1558*	17
In	155 $\pm$ 10	31.8×10^{-6}	2615 $\pm$ 125	2640*	17
Re	84 $\pm$ 4	2.3×10^{-6}	694 $\pm$ 28	622[a]; 799[b]	17

* Errors are reported to be less than 5%.

a This is the measured effective value for natural rhenium.

b This is the calculated effective value for natural rhenium.

** The area of each of these foils was 0.314 cm^2.

<u>All the reported results include the 1/v components.</u>

It is seen from Table II that the thicknesses of the foils are not the same in all cases. This, of course, introduces errors in the self-shielding factor, Q(t). The exact order of magnitude of this error is not known and workers in this field

tend to overlook it. A qualitative evaluation shows that the cadmium ratio as a function of thickness is essentially flat for foils of thicknesses below 100 Angstroms.

Another source of error is the uncertainty in the values of the thermal activation cross sections. A third source of error would be whether the epithermal neutron spectrum is $\frac{1}{E}$ or not. These sources of error along with the errors associated with the counting equipment complicate the error analysis.

The errors reported in Table II are based on the statistical deviation from the mean.

The results reported here agree well with the results of other workers for the indium resonance integral. The rhenium RI is significantly higher than that given in Ref. 17. However, it is in better agreement with the theoretical value than the earlier data.

REACTIONS WITH 14.1 Mev NEUTRONS

A study of specific interactions of 14.1 Mev neutrons with rhenium was made. These interactions include $Re^{185}(n,p)W^{185}$, $Re^{187}(n,p)W^{187}$, $Re^{185}(n,\alpha)Ta^{182}$, $Re^{187}(n,\alpha)Ta^{184}$, $Pe^{185}(n,2n)Re^{184}$, and $Re^{187}(n,2n)Re^{186}$.

Theoretical

J. Riddell[18], utilizing Levy's empirical mass formula, gives the binding energies of neutrons, protons and alpha particles as a function of mass number. Multiplying Riddell's values of binding energies by $\frac{(A+1)}{(A)}$ to convert to threshold energies for the above reactions, one obtains the values listed in Table III.

TABLE III

THRESHOLD ENERGY

Isotope	Threshold Energy, Mev		
	n,2n	n,p	n, α
Re^{185}	7.955	5.488	-1.843[a]
Re^{187}	7.627	6.029	-1.416[a]

[a] These values correspond to binding energy of alpha particles in parent nucleus.

Table III shows that it is possible for either Re^{185} or Re^{187} to decay by alpha emission if there were no potential barrier. According to D. J. Hughes[19] the potential barrier, B, can be expressed as

$$B = \frac{zZe^2}{r} \text{ ergs} = .96\ zZ/A^{1/3} \text{ Mev}, \qquad (6)$$

where z = 2 for alpha particles,

Z = nuclear charge of final nucleus,

e = electronic charge, and

r = the radius of the nucleus.

The height of the potential barrier for alpha transmission is about 24.6 Mev. The penetrability of this barrier by alpha particles with energy less than 18 Mev, according to the graphical results given by Hughes[19] is zero. Thus, it is apparent that neither naturally occurring alpha emission nor the (n, α) reaction with 14 Mev neutrons can take place with either Re^{185} or Re^{187}.

The height of the potential barrier for proton transmission in Re^{187} is 12.55 Mev. The probability of a proton, from the (n,p) reaction with 14 Mev neutrons, crossing this barrier is less than 0.1 according to Hughes.[19] Thus, it is clear that the (n,p) reaction with 14 Mev neutrons, is not very probable. Experimentally[20], no evidence of the (n,p) reaction was observed when a foil of rhenium was irradiated in the center of the UFTR and chemical separation was used to isolate Wolfram. A. S. Gillespie, Jr. and W. W. Hill[21] have used a cross section for the $Re^{187}(n,p)W^{187}$ reaction of 0.004 $\pm$ 0.004 barns.

Based on the formalism and curves of Blatt and Weisskopf[22] the Re(n,p)W cross section is given by

$$\sigma(n,p) = \sigma_c(n) \frac{F_p(E+Q_{np})}{F_n(E) + F_p(E+Q_{np}) + F_{n\alpha}(E+Q_{n\alpha})} \qquad (7)$$

where $\sigma_c(n)$ = neutron capture cross section

Q_{np} = 5.488 Mev

E = 14.1 Mev

$Q_{n\alpha}$ = -1.843 Mev.

The values of the F functions were obtained from Reference (22) p. 272. $\sigma_c(n)$ is also given on page 348 of Reference (22). Thus, the cross sections, σ (n,p) for 14.1 Mev neutrons is found to be 32.2 millibarns. Blatt and Weisskopf warn that this calculation could be in error by a factor of 10. Therefore, this value of σ (n,p) is not to be taken as exact, but merely indicates the order of magnitude.

The potential barrier is not involved in the (n,2n) reaction. The expression for the cross section of this reaction, as given by P. R. Byerly, Jr.[23], is

$$\sigma\,(n,2n) \approx \pi R^2 \left[1 - \left(1 + \frac{\epsilon_c}{\theta}\right) e^{-\epsilon_c/\theta} \right] \qquad (8)$$

where R = nuclear radius = $1.5 \times 10^{-13} A^{1/3}$ cm,

ϵ_c = excess of energy of the incident neutron over the threshold of the (n,2n) reaction, and

θ = is the temperature which determines the Maxwellian distribution of the neutrons emitted.

Figure 6 shows σ (n,2n) as a function of energy as calculated by Eq. (8) for Re^{187}. The values of θ used here were extrapolated from those given by Byerly. A very similar plot would be obtained for Re^{185}.

Experimental.-- The (n,2n) cross sections of Re^{185} and Re^{187} were determined. Separated isotopes of Re^{185} and Re^{187} were irradiated with 14.1 Mev neutrons obtained from a Texas Nuclear neutron generator.[24] Gold foils were used as a standard.

Four gold foils were placed against the tritium target in four quadrants and irradiated for two hours. Since the target and foils were surrounded by a 2 ft. water jacket for shielding purposes, it was necessary to cover the gold foils with a 10 mil indium foil, 6 mil gold foil and 35 mil cadmium foil. These three foils provided a good shield to filter out thermal and resonance neutrons produced in the water jacket. Subsequent analysis of the activity of the four gold foils showed that the neutron flux is symmetric only along the horizontal axis. Furthermore, the half-lives of each of these foils were about 14* hrs. and 5.3 days. These half-lives correspond to the $Au^{197}(n,2n)Au^{196}$ reaction, which indicates the absence of thermal and resonance neutron activation.

The rhenium samples were irradiated in a similar manner. A gold foil (101.28 mg) and a Re^{187} (36.3 mg) were placed against the tritium target along the horizontal axis and irradiated for two hours. The beam current to the target was about 200 micro-

* The half-life of Au^{196m} was later determined to be 10.4 ± 1 hrs.

amps. The same procedure was repeated with the Re^{185} (37.1 mg) sample. The purity of the Re^{187} and Re^{185} samples was 96.7 weight % and 96.8 weight % respectively. The impurity in the Re^{187} sample was Re^{185} and the opposite is true for the Re^{185} sample.

All samples were counted in a NaI(Tl) well type crystal. The crystal was 1 3/4 in. in diameter by 2 in. thick. The size of the well was 21/32 in. in diameter by 1 35/64 in. deep. The efficiency of this detector was measured to be 65%[25] for 0.411 Mev gamma rays. From this efficiency an effective length was calculated by the relation

$$0.65 = 1 - e^{-\mu(E)X} \tag{9}$$

where $\mu(E)$ is the total attenuation coefficient for gamma rays of energy E = 0.411 Mev, X is the effective length of the crystal. With this effective length the efficiency of the crystal for 0.343 Mev, corresponding to the average energy of gamma rays emitted by Au^{196}, was calculated to be 71 percent. The efficiency of the crystal for 0.137 Mev gamma rays was calculated to be 90%. This number corresponds to the ratio of the photons going through the crystal to the photons emitted in all direc-

tions. Over 99.9% of the photons entering the crystal produce pulses. A correction for the absorption of gamma rays in the aluminum can around the crystal was made.

Treatment of Data

Gold.-- The $Au^{197}(n,2n)Au^{196}$ reaction with 14.1 Mev neutrons yields one excited state of Au^{196} and a ground state of the unstable Au^{196} nucleus. It was not known how the Au^{196} in the excited state decays. Hollander, Perlman, and Seaborg[4] reported that this mode of decay proceeds either via isomeric transition or by electron capture. In order to ascertain the mode by which the excited Au^{196} decays, the decay rate was studied as a function of time. If Au^{196m} decays by electron capture, then the decay of Au^{196} is independent of the decay of Au^{196m} and the half-life of the two states can be easily determined by the process of stripping. It was found that this is not the case. In order to ascertain that Au^{196m} decays by isomeric transition to Au^{196}, the decay rate of Au^{196} and Au^{196m}

---

m Indicating the metastable state

should obey the relation

$$Y = A_e\, e^{-\lambda_e t} + \frac{\lambda_s A_e}{\lambda_s - \lambda_e} \quad e^{-\lambda_e t} - e^{-\lambda_s t} + B_s e^{-\lambda_s t} \tag{10}$$

where the subscripts e and s refer to Au^{196m} and Au^{196} respectively. The other symbols are:

Y = counting rate,

$A_e = \lambda_e N_e$, N = number of atoms,

$B_s = \lambda_s N_s$.

The quantities A_e and B_s were determined as follows. Let

$$G(A_e, B_s) = \sum_{i=1}^{n} (Y_i - Y_i')^2 \tag{11}$$

where Y_i' represents the right hand side of Eq. (10). Differentiating $G(A_e,B_s)$ with respect to A_e and B_s and setting the result equal to zero, one gets

$$\begin{aligned} &\sum_{i=1}^{n} Y_i \left[e^{-\lambda_e t_i} + \frac{\lambda_s}{\lambda_s - \lambda_e} \left[(e^{-\lambda_e t_i} - e^{-\lambda_s t_i}) \right] \right] \\ &= \sum_{i=1}^{n} A_e \left[e^{-\lambda_e t_i} + \frac{\lambda_s}{\lambda_s - \lambda_e} \left\{ (e^{-\lambda_e t_i} - e^{-\lambda_s t_i}) \right\} \right]^2 \\ &+ \sum_{i=1}^{n} B_s\, e^{-\lambda_s t_i} \left\{ e^{-\lambda_e t_i} + \frac{\lambda_s}{\lambda_s - \lambda_e} \quad (e^{-\lambda_e t_i} - e^{-\lambda_s t_i}) \right\} \end{aligned} \tag{12}$$

and

$$\sum_{i=1}^{n} Y_i \, e^{-\lambda_s t_i} = \sum_{i=1}^{n} A_e \left\{ e^{-(\lambda_e + \lambda_s)t_i} + \frac{\lambda_s}{\lambda_s - \lambda_e} \left(e^{-\lambda_e t_i} - e^{-\lambda_s t_i} \right) e^{-\lambda_s t_i} \right\} + \sum_{i=1}^{n} B_s e^{-\lambda_s t_i} \; . \qquad (13)$$

Ten experimental points were used in Equations (12) and (13) to determine A_e and B_s, assuming $\lambda_e = 0.0495 \text{ hr}^{-1}$ and $\lambda_s = .005396 \text{ hr}^{-1}$ corresponding to half-lives of 14 hrs.** and 5.3 days. Using the values for A_e and B_s in Equation (10) and calculating Y for various times, t, it was found that the experimental points obey Equation (10), thus proving that Au^{196m} decays by isomeric transition to Au^{196}. The study of the decay scheme of Au^{196} and Au^{196m} is shown in Appendix A.

Rhenium-187.-- Since there was a water jacket around the sample and standard, it was expected that some thermal and resonance activation would take place. Thus Re^{186} was produced by the (n,2n) reaction from Re^{187} and by the (n, γ) reaction from the 3.3% Re^{185} impurity present in Re^{187}. Also Re^{188} was

---

** This half-life was determined later to be 10.4 ± 1.0 hours.

produced by the (n, γ) reaction from Re^{187}. The production of Re^{184} by the (n,2n) reaction from Re^{185} was ignored because it was within the statistical fluctuations associated with the counting.

The activity of the sample was followed for 240 hours. From this study it was established that the decay rate of the rhenium sample corresponded to half-lives of 17 hours and 90 hours. These half-lives are associated with Re^{188} and Re^{186}. Based on the production of Re^{188} and the thermal activation cross sections of Re^{187} and Re^{185}, a correction was applied to subtract the amount of Re^{186} produced by the (n, γ) reaction of Re^{185}. The activity of Re^{186} that was produced by the (n,2n) reaction was then divided by 0.231, the fraction of gammas per disintegration, and by the efficiency of the crystal to obtain the absolute activity.

Rhenium-185.-- The $Re^{185}(n,2n)Re^{184}$ reaction with 14.1 Mev neutrons also results in an excited state of Re^{184m} whose half-life is 2.2 days, and a ground state with a half-life of 50 days. Again it is not known if Re^{184m} decays by isomeric transition or by electron capture. It was assumed that it decays by electron capture and the test used on gold above was applied to Re^{184m}. It was found that the equation of the line

$$Y = A_e e^{-\lambda_e t} + B_s e^{-\lambda_s t} + C_r e^{-\lambda_r t} \quad (14)$$

where

Y = counting rate,

$A_e = \lambda_e N_e$ for Re^{184m},

$B_s = \lambda_s N_s$ for Re^{184},

$C_r = \lambda_r N_r$ for Re^{186},

agrees with the experimental points. In Equation (14) the production of Re^{188} from Re^{187} (impurity in Re^{185}) by the (n, γ) reaction was ignored because Equation (14) was applied to the data after 190 hours from the time of irradiation. This allows more than 10 half-lives for Re^{188} to decay out. The decay scheme of Re^{184} and Re^{184m} is shown in Appendix B.

Results

Figure 7 shows the decay rate as a function of time for the gold irradiated with the Re^{187} sample. The half-life of Au^{196} was found by least squares fit to be 5.3 days. The half-life of Au^{196m} was assumed to be 14*hours and this excited level decays by isomeric transitions to Au^{196}.

Figure 8 shows the decay rate of Re^{188} and Re^{186}. A least squares fit of the linear portion of the data gives a half-life

* This half-life was later found to be 10.4 ± 1 hrs.

of 90 hours corresponding to the half-life of Re^{186}. The half-life of the residue after stripping was 17 hours corresponding to that of Re^{188}.

Paul and Clarke[26] reported a cross section for the $Au^{197}(n,2n)Au^{196}$ reaction with the 5.3 day half-life as 1.722 $\pm$ 0.465 barns. Using this cross section and the 5.3 days activity of the gold and the Re^{186} activity due to the (n,2n) reaction with Eq. (1), a σ (n,2n) cross section for Re^{187} was calculated to be 1.44 $\pm$ 0.41 barns.

Figure 9 shows the decay rate <u>vs</u>. time for the Re^{184}, Re^{184m} and Re^{186} irradiated with gold. The σ (n,2n) cross section for Re^{185} was calculated to be 1.91 $\pm$ 0.6 barns. The σ (n,2n) cross section for the $Re^{185}(n,2n)Re^{184m}$ was found to be 1.12 $\pm$ 0.4 barns. Table IV summarizes the results of the (n,2n) cross section experiments.

The agreement between the values of the σ (n,2n) reported here and those reported by other workers is within statistical error.

CAPTURE GAMMA RAYS

Work on measuring the prompt gamma rays emitted when thermal neutrons interact with rhenium is being done at the present. Here, however, the work of Groshev <u>et</u>.<u>al</u>.[29] is reported. These inves-

TABLE IV

CROSS SECTION, σ (n,2n), IN BARNS FOR 14.1 MEV NEUTRONS

Reaction	This Work 14.1 Mev	Ashby et.al.[27] 14.1 Mev	Paul & Clarke[26] 14.5 Mev	Khurana & Hans[28] 14.8 Mev
$Au^{197}(n,2n)Au^{196}$**		$2.6 \pm 0.20^{(a)}$	$1.722 \pm 0.465^{(b)}$	-
$Re^{187}(n,2n)Re^{186}$	1.44 ± 0.41	-	-	1.67 ± 0.16
$Re^{185}(n,2n)Re^{184}$	1.91 ± 0.60	-	-	-
$Re^{185}(n,2n)Re^{184}$	1.12 ± 0.4	-	-	-

** Standard, which was taken as 1.722 ± 0.465

a Represents the sum of the cross sections, $Au^{197}(n,2n)Au^{196}$ and $Au^{197}(n,2n)Au^{196*}$

b Represents the cross section, $Au^{197}(n,2n)Au^{196}$

tigators used a magnetic Compton Spectrometer with a resolving power of 2 percent. Thermal neutrons were obtained from the RFT Reactor at the U.S.S.R. Academy of Sciences Atomic Energy Institute.

Figure 10 shows the corrected spectrum obtained by Groshev et. al. Values of H_p and a factor of 1×10^4 were applied to the data in Figure 10 to yield the spectrum plotted in Figure 11. The data in Figure 11 were integrated to yield the number of photons emitted in various energy intervals per 100 neutrons captured. These data are shown in Table V. Troubetzkoy and Goldstein[30] also reworked these same data, and their conclusions are included in Table V.

TABLE V

GAMMA PHOTONS - THERMAL NEUTRON
CAPTURE - RHENIUM

Energy Interval, Mev	This Work	Photons/100 Captures Reference 30
0.55-1.0	58	
0.0-1.0		124
1.0-2.0	88	88
2.0-3.0	60	62
3.0-5.0	49.2	51
5.0-7.0	7.2	10.5
7.0-9.0	0	0
9.0	0	0

Discrete gamma rays were also tabulated by Groshev et.al.[29], and their table is reproduced below.

RHENIUM CAPTURE GAMMA RAYS
(Groshev et.al.[a])

Number of Line	Emitting Isotope	E_γ, Mev	I
1	Re^{186}	6,14 (3)	0,4
2	Re^{188} ?	5,94 (2)	1,8
3	-----	5,57 (5)	0,4
4	-----	5,30 (4)	0,6
5	-----	5,10 (3)	1.6

a) previously unpublished.

ELASTIC AND INELASTIC SCATTERING

Although no measurements on the elastic and inelastic scattering cross sections were made, a technique for separating gamma-ray pulses from neutron pulses in NaI(Tl) crystal was developed for that purpose. This technique appears in Appendix C.

COMPARISON OF SHIELDING PROPERTIES OF RHENIUM AND LEAD FOR THERMAL NEUTRONS

A calculation comparing the shielding properties of rhenium and lead for thermal neutrons was made. A slab of rhenium, 34 cm. thick, and a slab of lead, 61.55 cm. thick, were chosen. The thickness of each slab corresponded to a surface density of 698 gm/cm^2 as recommended by Price, Horton and Spinney(31) for a typical reactor.

In order to calculate the gamma rays produced by neutron absorption in a material and transmitted through the material, the following assumptions were made:

(1) A collimated beam of one neutron per second per cm^2 is incident on the slab,

(2) Neutron scattering out of the beam is equal to neutron scattering into the beam,

(3) Thermal neutron absorption will result in gamma-ray emission, and

(4) The gamma-ray emission is isotropic

With these assumptions, the number of gamma rays of energy E per cm^2 per second emerging from the rear face of the slab along the axis of the beam can be expressed as

$$Y(E) = V(E) \int_{X=0}^{X=L} \frac{B\, \phi_o e^{-\Sigma_a X}\, e^{-\mu_o(E)\,[L-X]}\, \Sigma_a dX}{4\pi\, (L + \epsilon - X)^2} \qquad (15)$$

In Equation (15)

Y(E) = the gamma-ray flux emerging from the rear face of the slab and measured at a distance ϵ away from the slab along the axis of the initial neutron beam,

V(E) = the number of gamma rays of average energy E emitted per neutron absorption,

B = the gamma-ray buildup* factor defined as $B = Ae^{-\alpha_1 \mu_o(E)\,[L-X]} + (1-A)e^{-\alpha_2 \mu_o(E)\,[L-X]}$,

ϕ_o = the initial neutron flux on the front face of the slab,

---

* The definition of B is taken from H. Goldstein[32].

$e^{-\Sigma_a X}$ = the probability that a neutron will travel a distance X in the slab sithout being absorbed where Σ_a is the macroscopic absorption cross section,

$e^{-\mu_o(E)[L-X]}$ = the probability that a gamma-ray emitted after neutron absorption in dX about X will travel a distance L-X and emerge on the other side of the slab and $\mu_o(E)$ is the total attenuation coefficient of the material,

$\Sigma_a dX$ = the probability that a neutron will be absorbed in dX about X,

L = shield thickness, and

ϵ = distance from shield to detector.

Introducing the expression for B into Equation (15) gives

$$Y(E) = \frac{V(E)\phi_o \Sigma_a}{4\pi}\left\{\int_{X=0}^{X=L} \frac{A\, e^{-\Sigma_a X-\mu_o(E)[L-X][1+\alpha_1]}\, dX}{[L+\epsilon-X]^2} + (1-A)\int_{X=0}^{X=L} \frac{e^{-\Sigma_a X-\mu_o(E)[L-X][1+\alpha_2]}\, dX}{[L+\epsilon-X]^2}\right\} \tag{16}$$

If $\mu_o(1+\alpha_1) - \Sigma_a$ and $\mu_o(1+\alpha_2) - \Sigma_a$ are ≥ 0 then Equation (16) can be shown to become after integration[33]

$$Y(E) = \frac{V(E)\phi_o \Sigma_a e^{-\Sigma_a L}}{4} \left\{ Ae^{b_1\epsilon}\left[\frac{E_2(b_1 \epsilon)}{\epsilon} - \frac{E_2(b_1 [L+\epsilon])}{L+\epsilon}\right] \right.$$

$$\left. + (1-A)e^{b_2\epsilon} \quad \frac{E_2(b_2\epsilon)}{\epsilon} - \frac{E_2(b_2[L+\epsilon])}{L+\epsilon} \right\} \tag{17}$$

where $b_1 = \mu_o(1+\alpha_1) - \Sigma_a$ and $b_2 = \mu_o(1+\alpha_2) - \Sigma_a$. The values of the E functions have been tabulated by various authors[32]. Thus, for the case where $b_1 \geq 0$ and $b_2 \geq 0$, Y(E) can be calculated by Equation (17). If $b_1 < 0$ and $b_2 < 0$, then integration of Equation (16) gives

$$Y(E) = \frac{V(E)\phi_o \Sigma_a e^{-\Sigma_a L}}{4} \left\{ Ae^{-b_1\epsilon}\left\{ -\frac{1}{L+\epsilon} e^{b_1(L+\epsilon)} \right. \right.$$

$$+ 1/\epsilon \; e^{b_1\epsilon} + b_1 \left[\ln \frac{L+\epsilon}{\epsilon} + \frac{b_1 L}{1!} + \frac{b_1^2 \left[(L+\epsilon)^2 - \epsilon^2\right]}{2.2!} \right.$$

$$\left.\left. + b_1^3 \frac{\left[(L+\epsilon)^3 - \epsilon^3\right]}{3.3!} + \cdots + b_1^n \frac{\left[(L+\epsilon)^n - \epsilon^n\right]}{n.n!} \right] \right\}$$

$$+ (1-A)e^{-b_2\epsilon}\left\{ -\frac{1}{L+\epsilon} e^{b_2(L+\epsilon)} + \frac{1}{\epsilon}e^{b_2\epsilon} \right. \tag{18}$$

$$+ b_2 \left[\ln \frac{L+\epsilon}{\epsilon} + \frac{b_2 L}{1!} + \frac{b_2^2 \left[(L+\epsilon)^2 - \epsilon^2\right]}{2.2!} \right.$$

$$\left.\left.\left. + b_2^3 \frac{\left[(L+\epsilon)^3 - \epsilon^3\right]}{3.3!} + \cdots + b_2^n \frac{\left[(L+\epsilon)^n - \epsilon^n\right]}{n.n!} \right] \right\} \right\}.$$

The series in Equation (18) converges very slowly if L is > 30; consequently, graphical integration was used to evaluate the integrals.

Calculated Results--. Equation (17) was used to calculate Y(E) for an incident neutron beam of one neutron per second per cm^2 on a slab of lead 61.55 cm thick. The values of the constants A, α_1, and α_2 were taken from Reference (32). The values of $\mu_0(E)$ and V(E) were taken from References (34) and (30). Equation (18) was used to calculate Y(E) for a beam of one neutron per second per cm^2 incident on a slab of rhenium 34 cm thick. The values of A, α_1, and α_2 used were actually for wolfram, but since the density and atomic number of rhenium are not very different from those of wolfram, the use of these constants was justified. Table VI shows the values of Y(E) obtained from these calculations.

TABLE VI

CALCULATED VALUES OF Y(E) FROM Re AND Pb
PER NEUTRON PER SECOND PER CM^2

Energy, Mev	$Y(E)_{Re}$	$Y(E)_{Pb}$
0.5	2.647×10^{-52}	---
1.5	1.348×10^{-27}	---
2.5	2.917×10^{-25}	---
4.0	1.176×10^{-24}	---
6.0	1.927×10^{-25}	---
7.33	---	1.766×10^{-4}

The calculated results shown in Table VI indicate that secondary gamma-ray production is not a problem with a rhenium shield. Almost no thermal neutrons will leave the rhenium shield, but 70 percent of the neutrons will be transmitted through a lead shield. Previous calculations[2], which did not include the effects of secondary gamma-ray production, have shown that weight savings can be obtained with a rhenium shield. All of these factors show that rhenium offers great potential for reactor shielding. Results similar to the results shown in Table VI would be expected from epithermal neutrons because the resonance integral of rhenium is much greater than that of lead.

APPENDIX A

STUDY OF THE DECAY OF Au^{196} AND Au^{196m}

EXPERIMENTAL

A 97.2 milligram circular gold foil, was placed against the tritium target of the Texas Nuclear 14.1 Mev neutron generator[24]. The foil was irradiated for a period of two hours at a beam current of 250 microamps. The pulse-height spectrum of the gamma rays from the decay of Au^{196} and Au^{196m} was obtained with a 1 3/4" diameter x 2" long NaI(Tl) crystal and a multichannel analyzer. Frequent measurements of the pulse-height spectra were continued for 12 days.

Since 14.1 Mev neutrons can induce the (n,p) reaction in gold, a chemical separation which removed Pt^{197} from the sample was performed. The procedure utilized ethyl acetate extraction of the 6N hydrochloric acid solution of the gold foil which gives essentially complete decontamination from platinum radioactivities[35].

The foil was dissolved in aqua regia, platinum carrier was added and the solution was evaporated to dryness. The

---

^{m} Indicate metastable state of Au^{196}.

residue was taken up in 6N hydrochloric acid, mixed with an equal volume of ethyl acetate and shaken in a separatory funnel. After separation from the initial aqueous layer, the gold-bearing organic phase was washed with two additional volumes of 6N hydrochloric acid solution. The residue of the evaporation of the ethyl acetate solution was taken up in dilute nitric acid, transferred to a counting container and evaporated to dryness. Recovery of the gold radioactivity was found to be complete. A source prepared from the aqueous layer, which contained the platinum carrier, was found to be inactive.

Treatment of Data

The pulse-height distributions that were obtained for the foil after isomeric transition activity had decayed out were corrected back to a time at which the gamma rays from the isomeric transition were present in the pulse-height distributions. The difference between these two curves gave the pulse-height distribution caused by gamma rays from the isomeric transition alone. A plot of the count rate per channel in each peak versus time demonstrated that all of the residual peaks had the same half-life.

The intensity of the highest energy gamma ray from the

isomeric transition was determined from known values of the photofraction and the crystal efficiency. The intensities of the lower energy gamma rays were determined in a similar manner following the subtraction of pulses contributed to each photopeak from higher energy gamma rays.

Results

Figure 12 shows the pulse-height spectrum of the gold sample obtained immediately after irradiation. Figure 13 shows the pulse-height spectrum of the same sample taken six days after irradiation. It is seen in Figure 13 that the gamma rays emitted from the isomeric transition of Au^{196m} have decayed out. After subtracting the background from each channel, the count rate per channel in Figure 13 was multiplied by 2.16 ($e^{\lambda t} = 2.16$, where $\lambda = 0.131$ day^{-1} is based on the measured $T_{1/2} = 5.3 \pm 0.3$ days for Au^{196}, and where t is the time difference between the pulse-height spectrum shown in Figure 12 and that in Figure 13.) The background was added to the pulse-height spectrum that was obtained and the resulting spectrum was subtracted from the spectrum shown in Figure 12. The difference between these two spectra is shown in Figure 14. This difference is the pulse-height spectrum of the gamma rays emitted from the isomeric

transition of Au^{196m}. It is seen that there are six gamma rays (38 ± 6 Kev, 77 ± 6 Kev, 155 ± 6 Kev, 193 ± 6 Kev, 232 ± 6 Kev, 270 ± 6 Kev) associated with the isomeric transition. The uncertainty in the energy of each gamma ray line depends on the linearity of the multi-channel analyzer. A test of the analyzer showed that the instrument was linear with an uncertainty in energy of one channel width.

The method for the determination of the half-life of the isomeric transition was outlined in a previous section. Figure 15 shows a plot of the count rate at each peak versus time. An average value of the least squares fit for the half-life of all the gamma rays was found to be 10.4 ± 1.0 hrs.

The method for the determination of the absolute number of the photons of each energy was also described previously. Table VII shows the intensity of each gamma ray. The limit of the uncertainty in the absolute number of the photons of each energy is ± 5%. The primary source of error was in the estimation of the contributions from higher energy photons to the lower energy regions in the pulse-height spectrum. Table VII shows the absolute intensities of the detected gamma rays associated with the decay of Au^{196} and Au^{196m}.

Comparison of the gamma rays shown in Table VII with the

work of T. M. Kavanagh[36] and R. Van Lieshout et.al.[37] indicated that 38 Kev peak was the result of X-rays produced in the crystal by the iodine. The 77 Kev peak was produced by X-rays from the gold and 84 Kev gamma rays emitted from the decay of Au^{196m}. The 155 and 193 Kev peaks are due to gamma rays emitted from Au^{196m}.

TABLE VII

INTENSITIES OF THE GAMMA RAYS ASSOCIATED WITH THE DECAY OF Au^{196} AND Au^{196m}

Energy, Kev	Photon Intensity Per Unit Time	Half-life
38 ± 6	55 x 10^3	10.4 ± 1 hours
77 ± 6	525 x 10^3	10.4 ± 1 hours
155 ± 6	340 x 10^3	10.4 ± 1 hours
193 ± 6	274 x 10^3	10.4 ± 1 hours
232 ± 6	88 x 10^3	10.4 ± 1 hours
270 ± 6	73 x 10^3	10.4 ± 1 hours
337 ± 6	354 x 10^3	5.3 ± 0.3 days
356 ± 6	354 x 10^3	5.3 ± 0.3 days
429 ± 6	270 x 10^3	5.3 ± 0.3 days
514 ± 6	26 x 10^3	5.3 ± 0.3 days
693 ± 6	125 x 10^3	5.3 ± 0.3 days

The 232 and 270 Kev gamma rays were not seen by either Kavanagh[36] or Lieshout et.al.[37]. These peaks could be the result of summed coincidences between the 77 Kev and the 155 Kev gamma rays and between the 77 Kev and the 193 Kev quanta. However, the intensities of these peaks appear to be too large to be explained by summed coincidences. This discrepancy must await further work.

It has been reported[4] that there was no positron emission in the decay of Au^{196}. On a theoretical basis, the difference between the mass number of Au^{196} and that of Pt^{196} is 0.00122 AMU[38] or 1.138 Mev which makes positron emission possible. Figure 1 shows that 0.514 Mev gamma rays were detected. Since each positron results in two 0.511 Mev gamma rays, it is seen that the positron emission in the decay of Au^{196} is 1.7% of the total modes of decay. It is not known whether or not the positron carries away all the excitation energy. It was also found that Au^{196} decays by beta emission 35.3% of the time and by electron capture 63% of the time. The values reported by J. M. Hollander et.al.[4] for these modes of decay are 20% and 80%, respectively.

Figure 12 also shows a peak at 0.693 Mev. This indicates that after the Au^{196} nucleus captures an electron, the resulting

Pt^{196} atom de-excites by the emission of a photon of 0.693 Mev as well as by the emission of two photons (0.356 Mev and 0.337 Mev) in cascade. The decay scheme presented in the compilations of J. M. Hollander, et.al.shows these two photons in cascade but does not show the 0.693 Mev photon.

APPENDIX B

DECAY SCHEME OF Re^{184} AND Re^{184m}

It was ascertained previously[39] that Re^{184m} decays by electron capture with a 2.2 day half-life and it has been shown[40] that Re^{184} also decays by electron capture with a 50-day half-life. The daughter nucleus is ${}_{74}W^{184}$ and is an even-even nucleus. Thus, the excited states of ${}_{74}W^{184}$ need to be known since the ${}_{74}W^{184}$ resulting from the decay of Re^{184} and Re^{184m} is formed in many excited states[40] and decays by gamma emission.

Excited States of ${}_{74}W^{184}$.-- In calculating the excited states of ${}_{74}W^{184}$ the collective model of A. Bohr and B. Mottelson[41] was used. The energy levels of the rotational spectrum are given by the relation[42]

$$E = E_o + \frac{\hbar^2}{2J} \left[I(I+1)\right] - b \left[I(I+1)\right]^2 , \qquad (19)$$

where E_o = a constant depending upon the individual particle structure,

J = moment of inertia of the deformed ${}_{74}W^{184}$ nucleus

I = spin of the nucleus

$b\left[I(I+1)\right]^2$ = a term which accounts for the vibration-rotation coupling.

The factor b is usually considered constant; however, R. K. Sheline[43] carefully warns that there is no a priori reason to

expect this constancy. Indeed, if b is assumed constant the rotational level corresponding to the 4^+ state differs from the experimentally determined state by 2 Kev. Such a difference is within the experimental error; however, the difference for the level corresponding to the 8^+ state deviates as much as 40 Kev from the experimental value. If b is not considered constant but is calculated for the 2^+, 4^+ and 8^+ states from the experimental data[40] one finds that the plot of $\ell n(b)$ versus $\ell n(I)$ yields a straight line.

The value of $\frac{3\hbar^2}{J}$ for $_{74}W^{184}$ is given in Reference (42) to be 112 Kev. The first two excited states of $_{74}W^{184}$ corresponding to $I = 2^+$ and $I = 4^+$ are given in Reference (43) to be 111.20 Kev and 364.04 Kev respectively. These energy levels are in agreement with the experimental values reported by Gallagher et.al.[40] By plotting ℓnb versus ℓnI for $I = 2^+$ and 4^+ and extrapolating to $I = 6^+$ and 8^+ the energy levels shown in Table VIII are obtained.

TABLE VIII

ENERGY LEVELS OF ROTATIONAL STATES OF $_{74}W^{184}$

Spin	Energy, Kev
2^+	111.2
4^+	364.04
6^+	748.20*
8^+	1240.00

* This level is not known to exist.

According to R. K. Sheline[43], $_{74}W^{184}$ has a gamma vibrational band head at 904 Kev. The rotational bands built on this gamma vibrational band can be obtained by the relation[44]

$$E = \frac{\hbar^2}{2J}\left[I(I+1) - I_o(I_o+1)\right] \tag{20}$$

where I_o is the spin of the band head and in this case is 2. The energy levels built on the gamma vibrational band are calculated by Equation (20) and shown in Table IX.

TABLE IX

ROTATIONAL ENERGY LEVELS BUILT ON THE GAMMA VIBRATIONAL LEVEL OF $_{74}W^{184}$

Spin	Energy level (above 904 Kev)	Total Energy Level; Kev
3	112	1016
4	261	1165
5	448	1352
6	672	1576
7	933	1837

The energy levels calculated above account for most but not all the gamma rays associated with the decay of Re^{184} and Re^{184m}. Thus, one should investigate the possibility of a beta vibrational band at about 1001 Kev above the ground state of $_{74}W^{184}$. According to Sheline[43] the beta and gamma vibrational bands are related as follows:

$$E_{\beta} = \left[\frac{3/2 \quad (\hbar^2/2J)^3}{b' - \frac{1}{2} \frac{(\hbar^2)^3}{(2J)} \Big/ (E_{\gamma})^2} \right]^{1/2} \tag{21}$$

where b' is 2.12b (b defined previously) and E_{γ} = 904 Kev.

Through this relationship it is found that E_{β} = 966 Kev. Since Equation (21) is only approximate, it is felt that the assignment of a beta vibrational band at 1001 Kev is reasonable. At this point, we can account for all the experimentally observed gamma rays emitted in the decay of Re^{184}. Table X shows the experimentally observed[39] and theoretically calculated gamma rays.

Besides the gamma-ray lines listed in Table X, Wilkins, et.al.[45] reported a 43 Kev line associated with a half-life of 2.2 days. This line, as suggested by Gallagher, et.al.[40] is due to an Auger electron.

In Figure 16 the percentages of the intensity of each line are based on the data given in Reference[40]. The percentages of the three most intense lines are given, the sum of all the rest is about one percent.

TABLE X

COMPARISON OF EXPERIMENTALLY OBSERVED AND THEORETICALLY CALCULATED GAMMA RAYS FROM Re^{184} AND Re^{184m}

Initial and Final States		Expt. Gamma-Ray Energy; Kev	Theoretical Gamma-Ray Energy, Kev	Half-Life
(β vib)	(γ vib)	97 ± 0.38	97	50 d
(0,2+)	(0,0+)	111.20 ± 0.06	111	"
(0,8+)	(2,3+)	210.0 ± 20	224	"
(0,8+)	(β vib)	230.0 ± 20	239	"
(2,4+)	(2,2+)	250.0 ± 20	257	"
(0,4+)	(0,2+)	252.8 ± 0.1	253	"
(0,8+)	(2,3+)	330 ± 25	336	"
(2,2+)	(0,4+)	540 ± 40	540	"
(β vib)	(0,4+)	642.4 ± 0.6	637	"
(2,2+)	(0,2+)	792.7 ± 0.8	793	"
(β vib)	(0,2+)	895.2 ± 0.9	890	"
(2,2+)	(0,0+)	904.3 ± 0.9	904	"
(2,4+)	(β vib)	159.0[a]	160	2.2 day
(β vib)	(2,2+)	not observed but possible	97	2.2 "
(2,2+)	(0,0+)	" "	904	2.2 "

(a) Based on data reported in Nuclear Data Sheets 1960 and Reference[45].

The collective model accounts very well for all the gamma rays associated with Re^{184} and Re^{184m} which decay by electron capture with a half life of 50 days and 2.2 days.

The decay scheme of Re^{184} was recently studied by K. M. Bisgard, C. Sharp Cook, P. Hornshoj and A. B. Knutsen(46). Their level scheme differs slightly from the level scheme shown in Figure 16.

APPENDIX C

SEPARATION OF GAMMA-RAY PULSES FROM NEUTRON PULSES IN NaI(Tl) DETECTORS*

Suppose that a pulse-height distribution from a mixture of neutrons and gamma rays in narrow beam geometry has been obtained. The pulse-height distribution can be divided into bins of equal energy width. The total number of pulses per unit time in the highest bin, I_T^o, can be expressed as

$$I_T^o = I_{\gamma(E_i)}^o + I_{n(E_1)}^o + I_{n(E_2)}^o + \dots + I_{n(E_j)}^o \tag{22}$$

where $I_{n(E_1)}^o$, $I_{n(E_2)}^o$ .... and $I_{n(E_j)}^o$ are the pulses per unit time caused by neutrons of energy E_1, E_2, ... E_j respectively. $I_{\gamma(E_i)}^o$ are pulses per unit time caused by gamma rays of energy E_i. Since the measurement leading to the result in Equation (22) was done in narrow beam geometry, by inserting a slab of lead of known thickness in the beam, one obtains a relation similar to Equation (22) except for the superscript o.

$$I_T = I_{\gamma(E_i)} + I_{n(E_1)} + I_{n(E_2)} + \dots + I_{n(E_j)} \tag{23}$$

There are other relations that can be utilized. These relations are

---

* This work was published in "Transactions of the American Nuclear Society," Vol. 5, No. 1, p.204 (1962).

$$I_{n(E_1)} = I^{o}_{n(E_1)} e^{-\Sigma_T(E_1)X} \ldots;$$

$$I_{n(E_j)} = I^{o}_{(E_j)} e^{-\Sigma_T(E_j)X}, \tag{24}$$

and

$$I_{\gamma(E_i)} = I^{o}_{\gamma(E_i)} e^{-\mu(E_i)X}$$

where $\Sigma_T(E_j)$ is the total macroscopic cross section and $\mu(E_i)$ is the attenuation coefficient. The total cross section for lead is essentially constant for neutrons above 0.03 ev.[49] Thus, substituting (24) in (23) one gets

$$I_T = I^{o}_{\gamma(E_i)} e^{-\mu(E_i)X} + \left(e^{-\Sigma_T X}\right) \sum_{j=1}^{J} I^{o}_{n(E_j)} \tag{25}$$

where $\sum_{j=1}^{J} I^{o}_{n(E_j)}$ is the sum of all the I^{o}_{n}'s. Similarly, one can represent the pulses caused by the various neutrons in (22) by $\sum_{j=1}^{J} I^{o}_{n(E_j)}$. Equations (22) and (25) contain two unknowns, $I^{o}_{\gamma(E_i)}$ and $\sum_{j=1}^{J} I^{o}_{n(E_j)}$. They can easily be solved to obtain the pulses caused by gamma rays of energy E_i and the pulses caused by neutrons in the highest bin.

Having obtained $I^{o}_{(E_i)}$ for the highest bin one can from the data given by Berger and Doggett [48] synthesize a "tail" representing pulses due to Compton scattering. The bin and tail contents can now be subtracted from the rest of the pulse-height

distribution and the same procedure can be repeated for the next lower bin; this stripping process is continued until all bins have been utilized. The end result will produce a separated pulse-height spectrum for gamma rays and for neutrons.

This procedure was applied using a beam of gamma photons and neutrons from the University of Florida Training Reactor. Two sets of experiments were performed: in one set a standard Co^{60} source was inserted in the beam while in the second set only neutrons and gamma rays from the reactor were incident on the crystal. Each set was analyzed to give the gamma-ray contribution and the neutron contribution to the total pulse-height distribution. The difference in areas under the 1.33 Mev peak between the two sets was 9016 counts per minute. This difference for the 1.17 Mev peak was 9686 counts per minute. These values differed from the true values, as determined from the Co^{60} alone, by 8.4 per cent and 0.23 per cent, respectively. In view of the above assumption concerning the total macroscopic cross section, this agreement is satisfactory.

Figure 17 shows the separated gamma-ray pulse-height distributions taken with and without the Co^{60} source.

Figure 18 shows the separated neutron pulse-height distributions taken with and without the Co^{60} source.

BIBLIOGRAPHY

1. C. T. Sims, E. N. Wyler, G. B. Gains and D. M. Rosenbaum, "A Survey of the Literature on Rhenium," Battelle Memorial Institute, WADC Technical Report 56-319, June (1956).

2. W. C. Simpson and J. A. Wethington, Jr., "Comparative Weights of Equivalent Shields for Gamma Radiations," USA TRECOM 1(7-59), July (1959).

3. R. T. Overman and H. M. Clark, "Radioisotope Techniques," p. 285, McGraw-Hill Book Co., New York (1960).

4. D. Strominger, J. M. Hollander, and G. T. Seaborg, Rev. Mod. Phys., 30, 585 (1958).

5. S. H. Vegors, Jr., L. L. Marsden and R. L. Heath, "Calculated Efficiencies of Cylindrical Radiation Detectors," ID016370 (Sept. 1, 1958).

6. M. W. Jones, C. C. McMullen, I. R. Williams and S. V. Nablo, Canadian J. Phys., 34, 69 (1956).

7. R. L. Macklin, N. H. Lazar, and W. S. Lyon, Phys. Rev., 107, 504 (1957).

8. Overman and Clark, op. cit, p. 108.

9. "Nuclear Data Sheets," National Academy of Sciences, National Research Council, (1959).

10. M. E. Rose, "Internal Conversion Coefficients," North Holland Publishing Co., Amsterdam (1958).

11. L. Seren, H. N. Friedlander and S. H. Turkel, Phys. Rev., 72, 888 (1947).

12. L. V. Groshev, V. N. Lutsenko, A. M. Demidov, and V. I. Pelekhov, "Atlas of Gamma Ray Spectra from Radiative Capture of Thermal Neutrons," p. 16, Pergamon Press, New York (1959).

13. H. Pomerance, Phys. Rev., 88, 412 (1952).

14. V. S. Dzelepov and L. K. Peker, "Decay Schemes of Radioactive Isotopes," AECL 457 (July, 1957).

15. G. M. Jacks, "A Study of Thermal and Resonance Neutron Flux Detectors," DP-608 August (1961).

16. R. H. Ritchie and H. B. Eldrige, Nuclear Science and Engineering, 8, 300-311 (1960).

17. R. L. Macklin and H. S. Pomerance, "Resonance Capture Integrals," Proceedings of the International Conference on the Peaceful Uses of Atomic Energy, 5: 96-101, (1955).

18. J. Riddell, "A Table of Levy's Empirical Atomic Masses," AECL No. 339, July (1956).

19. D. J. Hughes, "Pile Neutron Research," Addison-Wesley Publishing Co., Inc., Cambridge 42, Mass. (1953).

20. John A. Wethington, Jr., R. A. Karam and C. A. Bisselle, "Fourth Quarterly Technical Progress Report on the Nuclear Properties of Rhenium," Sept. 8, 1960.

21. A. S. Gillespie, Jr. and W. W. Hill, "Sensitivities for Activation Analysis with 14 Mev Neutrons," Nucleonics Vol. 19, No. 11, p. 170 (1961).

22. J. M. Blatt and V. F. Weisskopf, "Theoretical Nuclear Physics," John Wiley & Sons, (1952).

23. Paul R. Byerly, Jr., "Fast Neutron Physics," Edited by J. B. Marrion and J. L. Fowler, Interscience Publishers, Inc., New York (1960).

24. R. A. Karam, T. F. Parkinson and F. J. Munno, "Ninth Quarterly Technical Report on the Nuclear Properties of Rhenium." March (1962).

25. A. A. Katterhenry, "Experimental Measurements of Thermal Neutron Density In and Around Detectors". Thesis, University of Florida, (1960).

26. E. B. Paul and R. L. Clarke, Can. J. Phys. Vol. 31, 267 (1953).

27. V. J. Ashby, H. C. Carton, L. L. Newkirk, and C. J. Taylor, Phys. Rev. Vol. 111, No. 2, 616 (1958).

28, C. S. Khurana and H. S. Hans, Nuclear Physics Vol. 28, No. 4, 560 (1961).

29. Groshev, Lutsenko, Demidov and Pelekhov, op. cit. p. 165

30. E. Troubetzkoy and H. Goldstein, Nucleonics, 18 (11), 171, (November, 1960).

31. B. T. Price, C. C. Horton, and K. T. Spinney, "Radiation Shielding," p. 279, Pergamon Press, London, (1957).

32. H. Goldstein, "Fundamental Aspects of Reactor Shielding," p. 353, Addison-Wesley Publishing Co., Inc., Reading, Mass. (1959).

33. J. A. Wethington, Jr., and R. A. Karam, "Fifth Quarterly Technical Report on the Nuclear Properties of Rhenium," March (1961).

34. E. Storm, E. Gilbert and H. Isreal, "Gamma-Ray Absorption Coefficients for Elements 1 Through 100," LA-2237, April 1957.

35. R. F. Emery, "The Radioactivity of Gold," Monograph Series on the Radiochemistry of the Elements, Nat'l. Res. Council, Nat'l. Acad. Sci., Nuclear Science Series, NAS-NS 3036 (1961).

36. T. M. Kavanagh, Can. J. Phys. Vol. 38, 1436 (1960).

37. R. Van Lieshout, R. K. Girgis, R. A. Ricci, A. H. Wapstra and C. Ythier, Physica 25, 703 (1959).

38. A. H. Wapstra, Isotopic Masses I & II, J. R. Huizenga, Isotopic Masses III, Physica XXI, 367 (1955).

39. R. A. Karam, T. F. Parkinson, F. J. Munno, and E. E. Menge, "Tenth Quarterly Technical Progress Report on the Nuclear Properties of Rhenium," June 8, (1962).

40. C. J. Gallagher, Jr., D. Strominger and J. P. Unik, Phys. Rev. 110, 725 (1958).

41. A. Bohr and B. R. Mottelson, KgC. Danske Videnshab Selskab 27 No. 16 (1953).

42. Alder, Bohr, Huus, Mottelson and Wither, Rev. Mod. Phys. 28, 432 (1956).

43. R. K. Sheline, Rev. Mod. Phys. 32, 1 (1960).

44. F. Everling, L. A. Koenig, J. H. E. Mattauch and A. H. Wapstra, 1960 Nuclear Data Tables, U. S. Atomic Energy Commission, Feb. (1961).

45. G. Wilkinson and H. G. Hicks, Phys. Rev. 77, 314 (1950).

46. K. M. Bisgard, C. Sharp Cook, P. Hornshoj and A. B. Knutsen, "Levels in W^{184} Populated in the Decay of Re^{184}," Submitted to Nuclear Physics, Sept. (1962).

47. D. J. Hughes and J. A. Harvey, "Neutron Cross Sections," BNL 325 (July 1, 1955).

43. M. J. Berger and J. Dogget, J. Research Nat'l. Bur. Standards 56, 355 (1956).

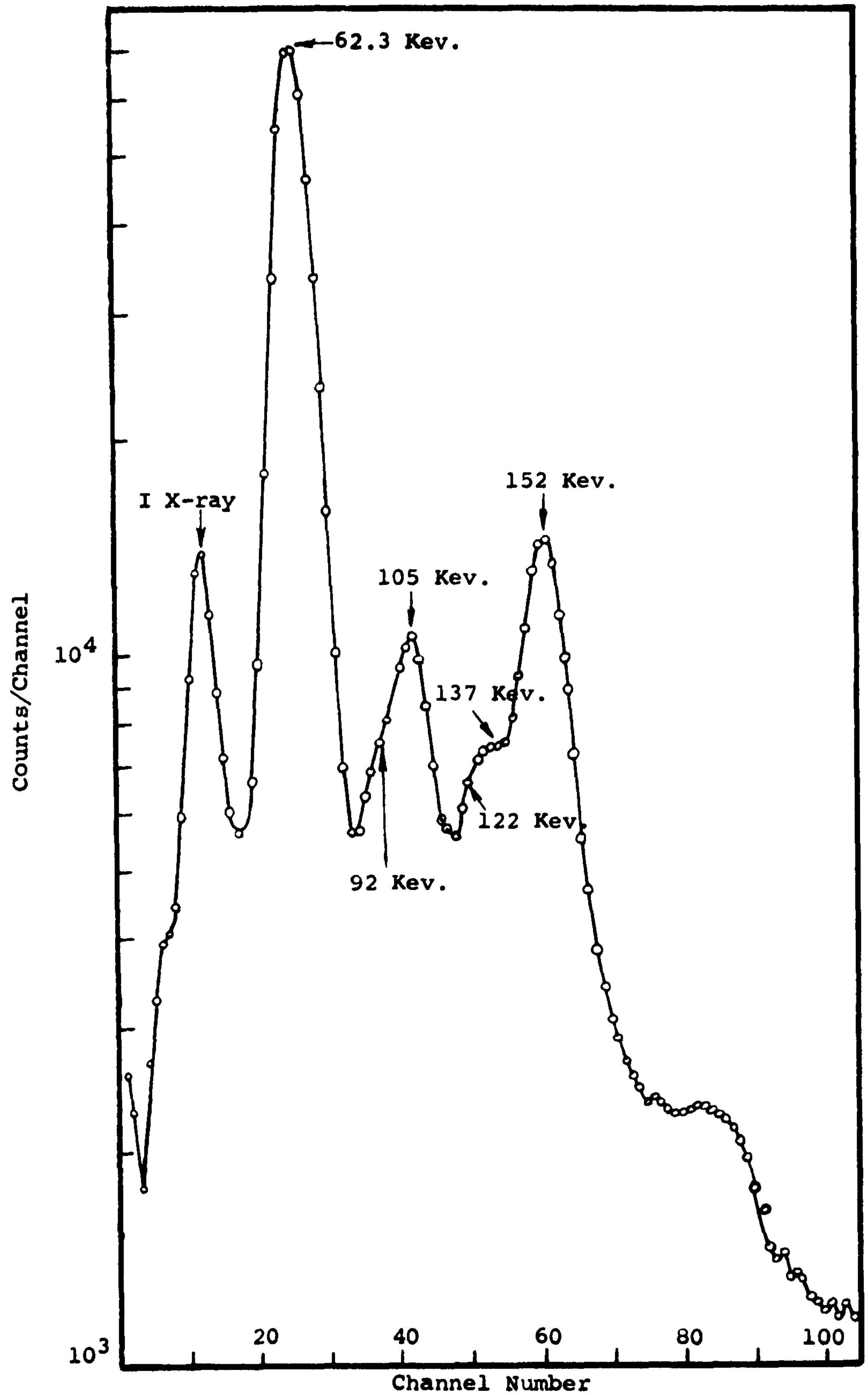

Fig. 1. Rhenium Pulse-Height Spectrum Thirteen Minutes After Irradiation.

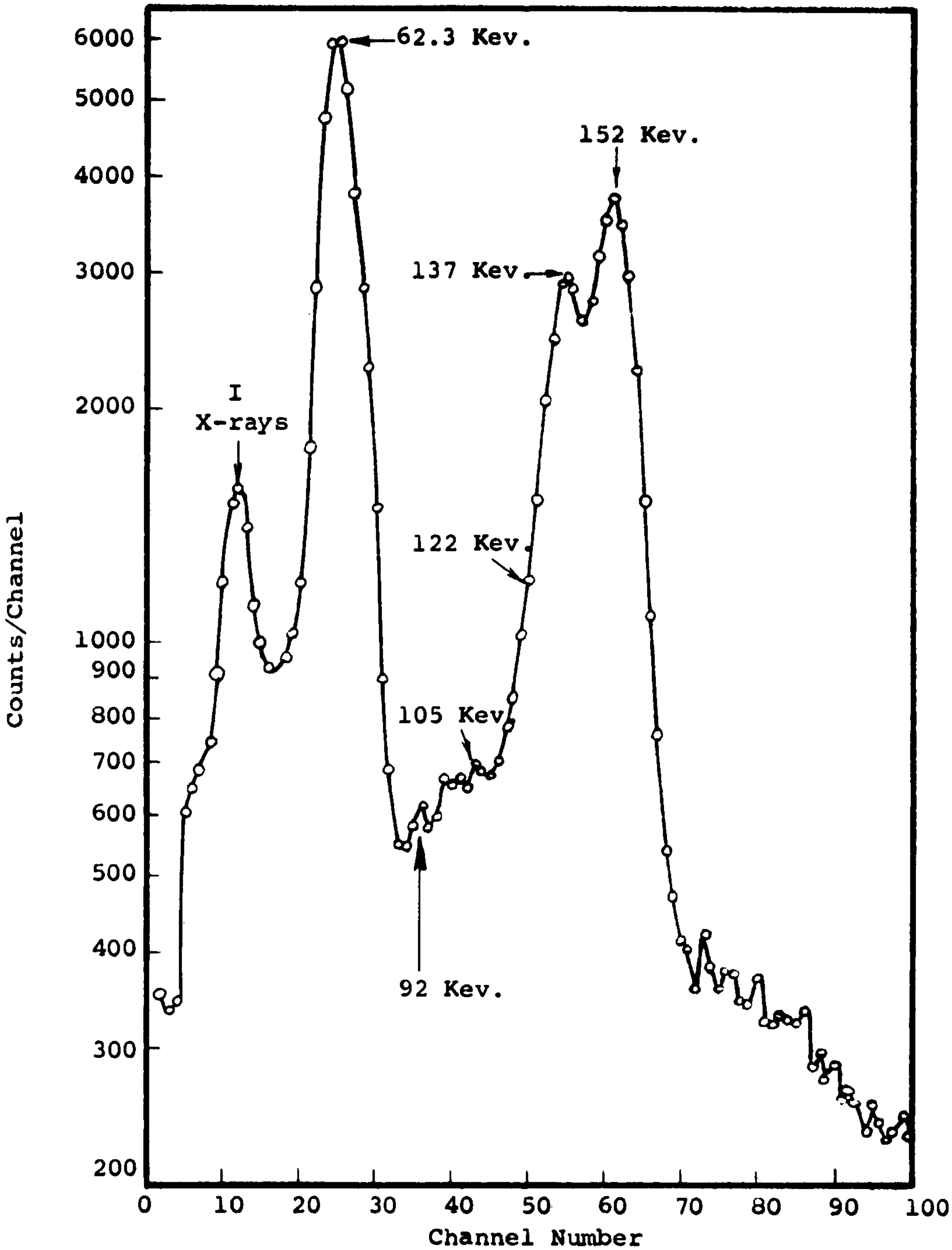

Fig. 2. Rhenium Pulse-Height Spectrum Fifty Four Hours After Irradiation.

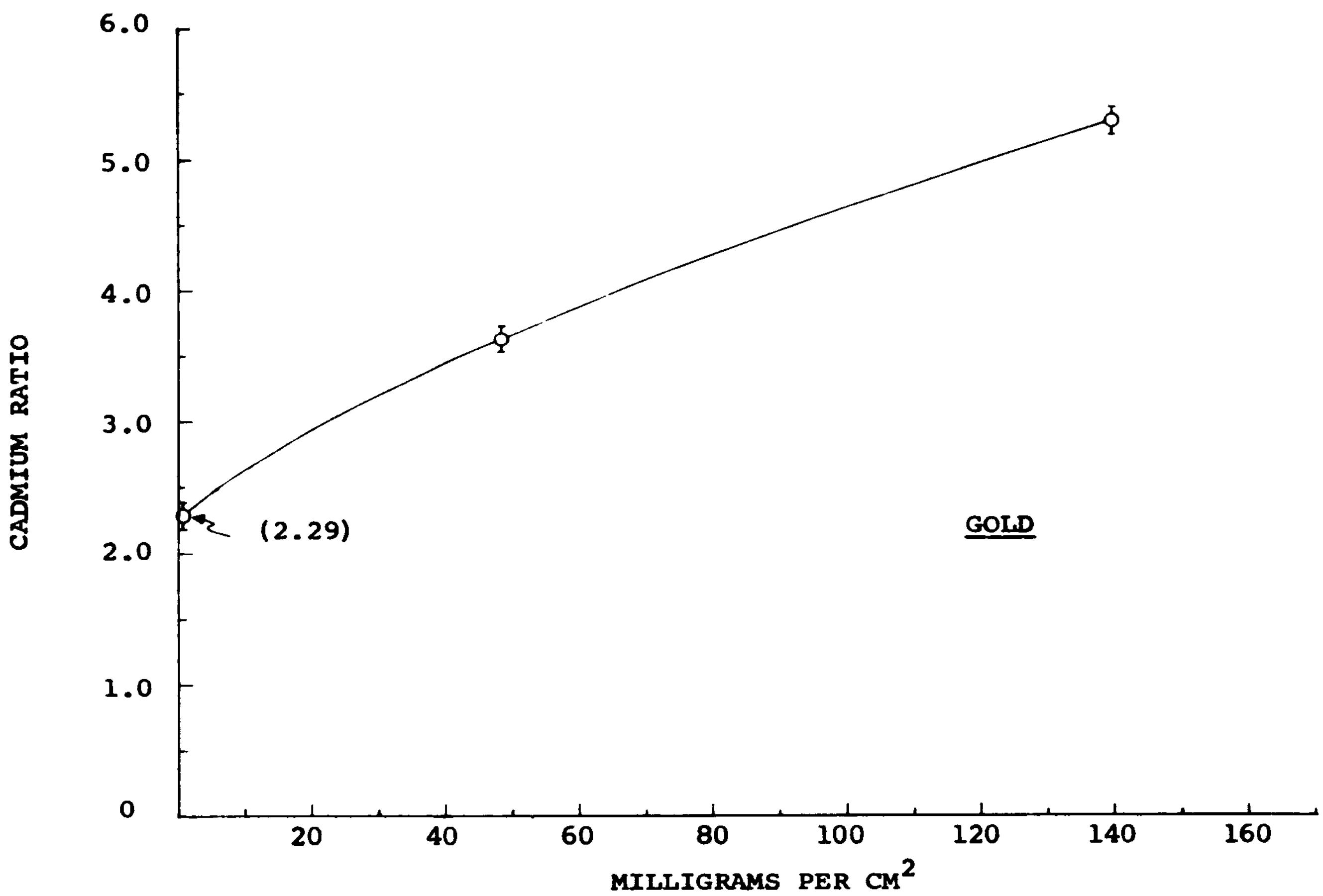

Figure 3. Gold Cadmium Ratio vs. Thickness

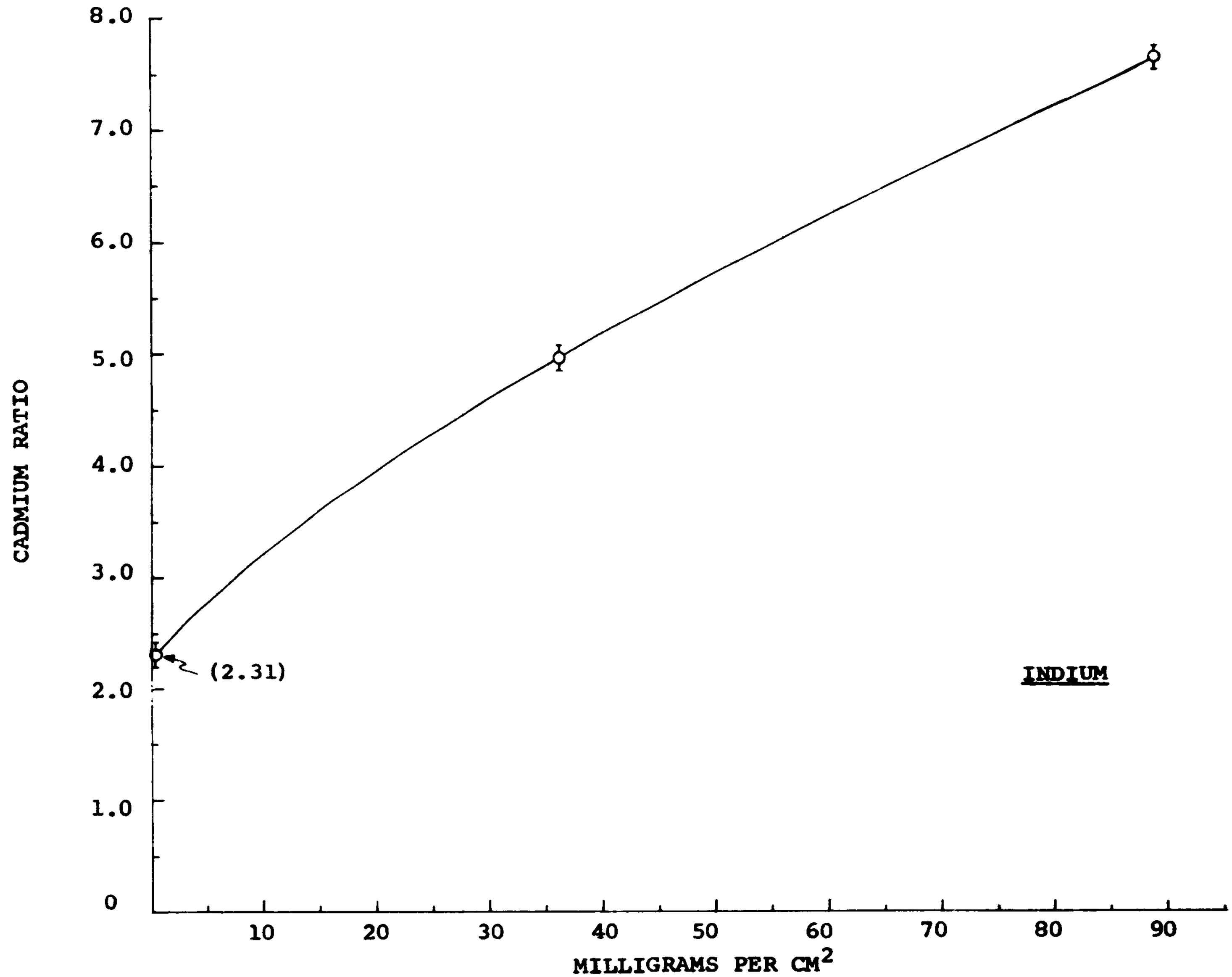

Figure 4 . Indium Cadmium Ratio vs. Thickness

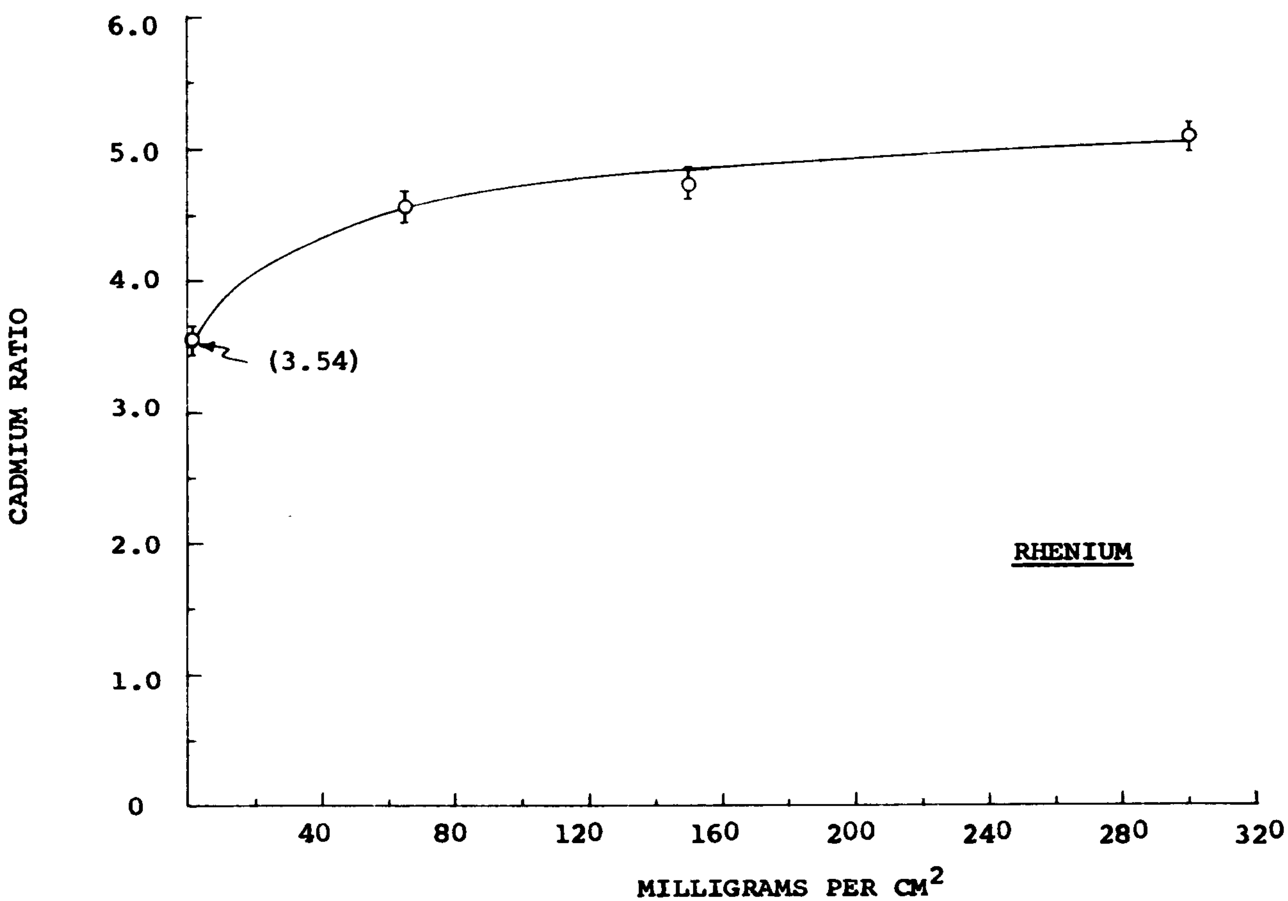

Figure 5. Rhenium Cadmium Ratio vs. Thickness

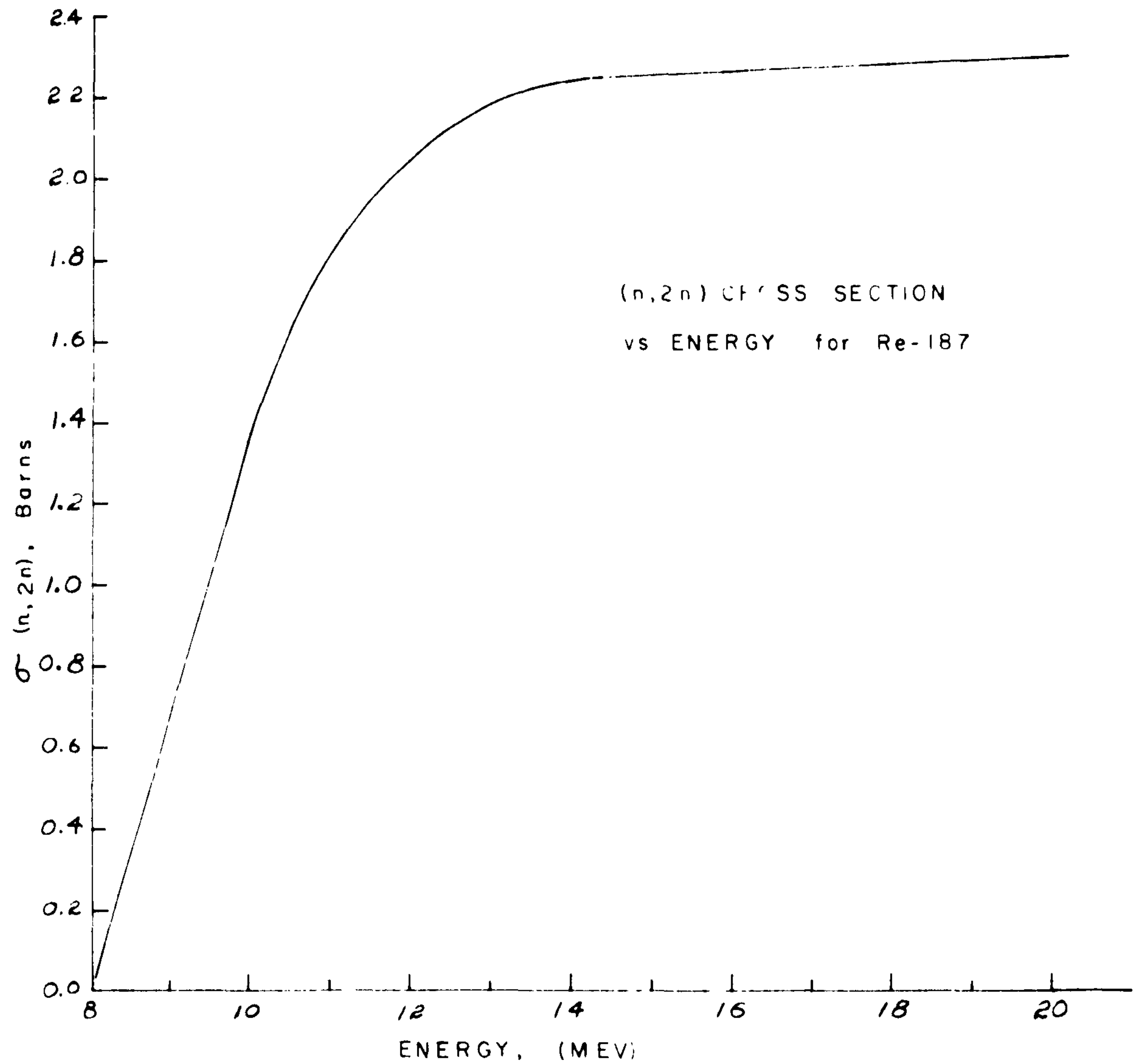

Figure 6. Cross Section of (n,2n) for Re^{187} as a Function of Energy

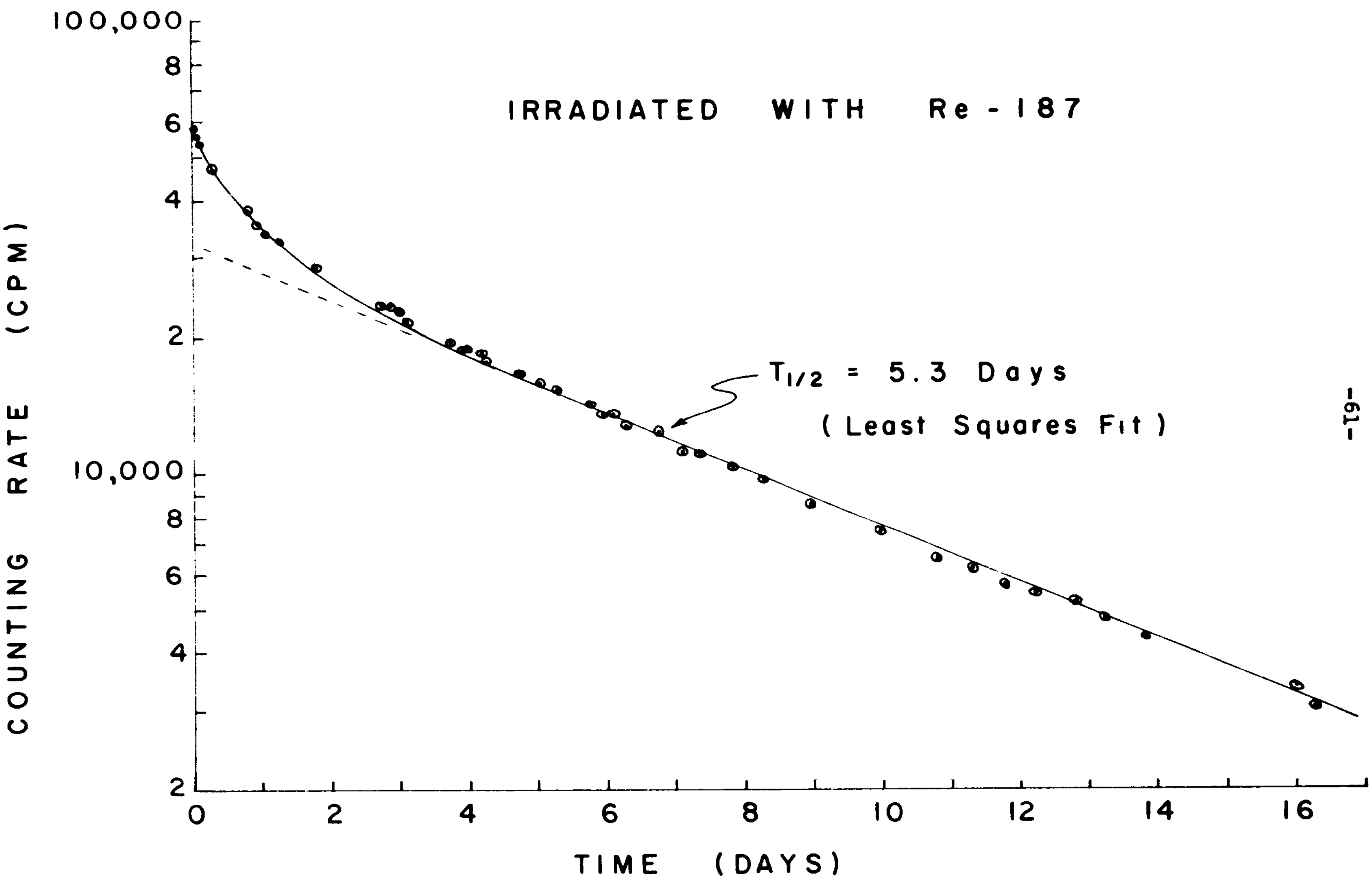

FIGURE 7 · DECAY OF GOLD

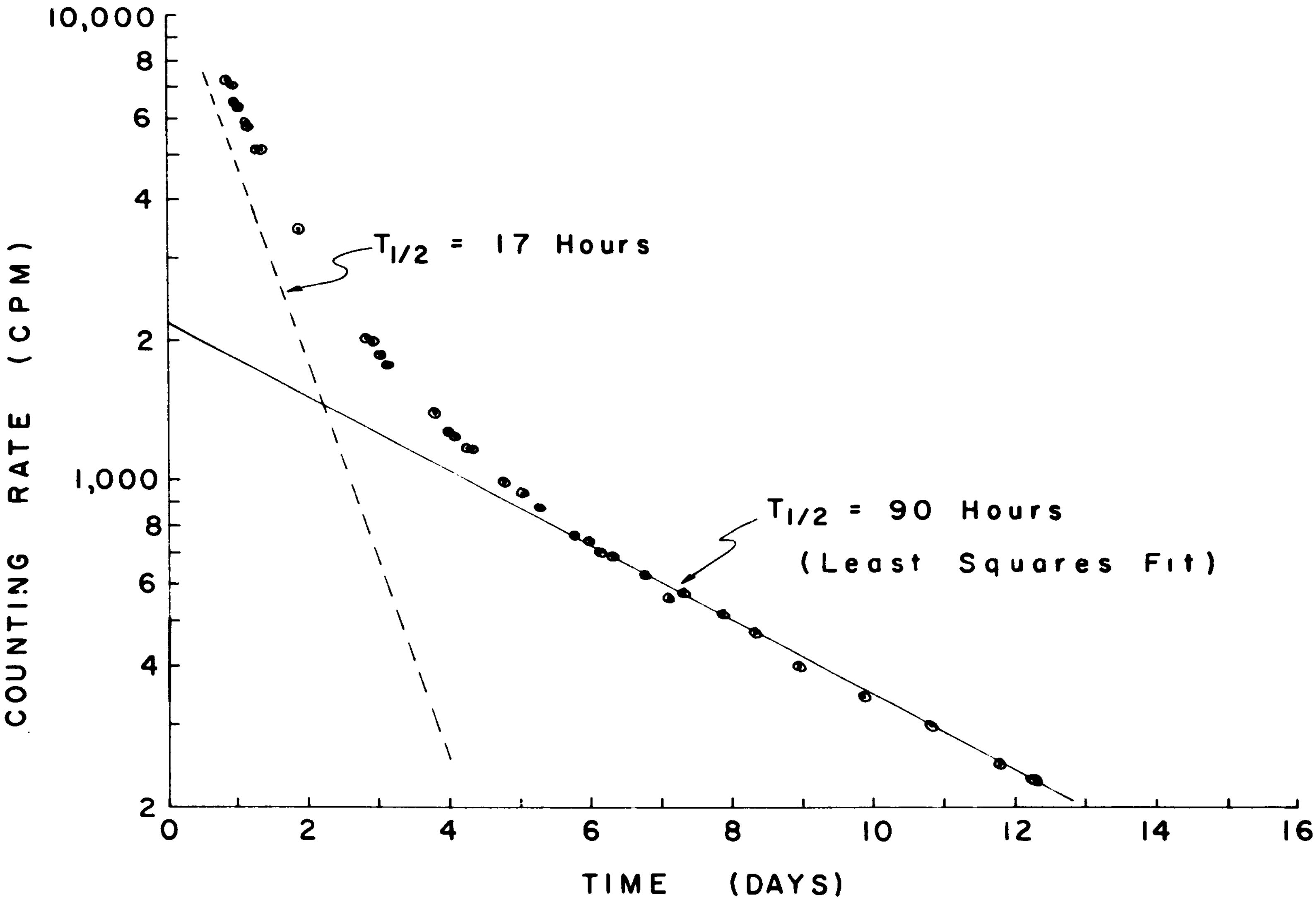

FIGURE 8 . DECAY OF Re - 187

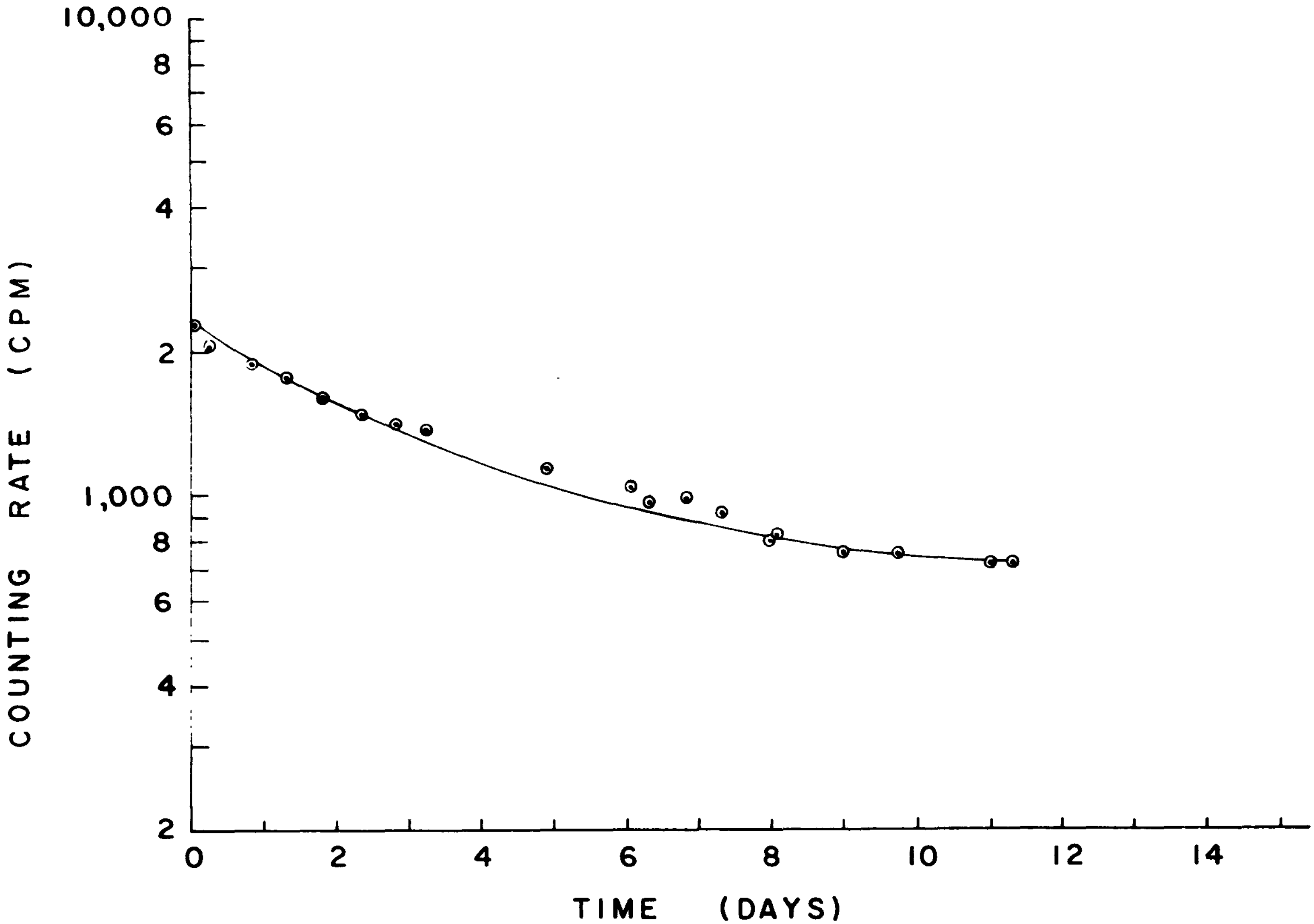

FIGURE 9 · DECAY OF Re-185

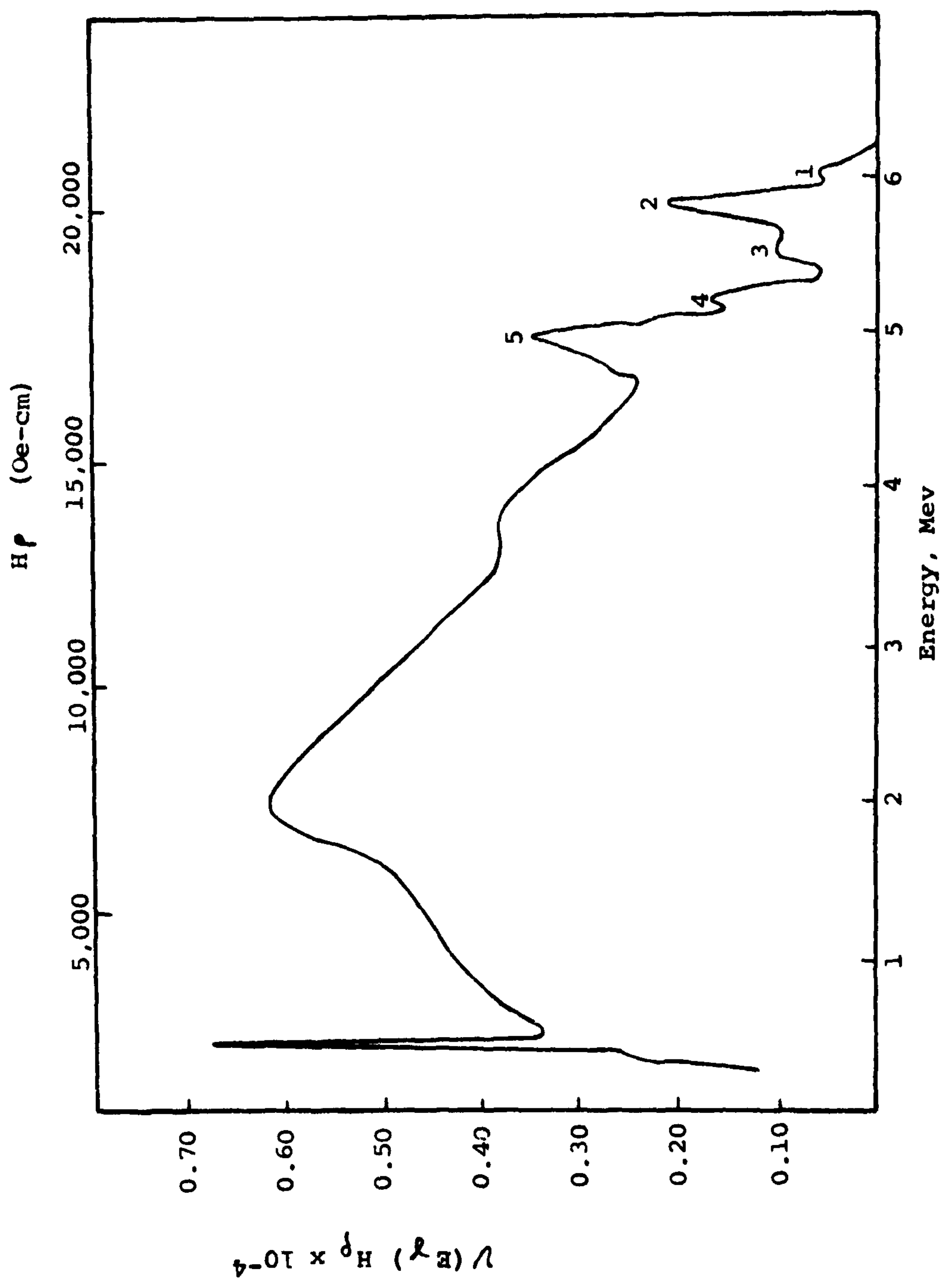

Figure 10. Corrected Spectrum of Rhenium Gamma Rays

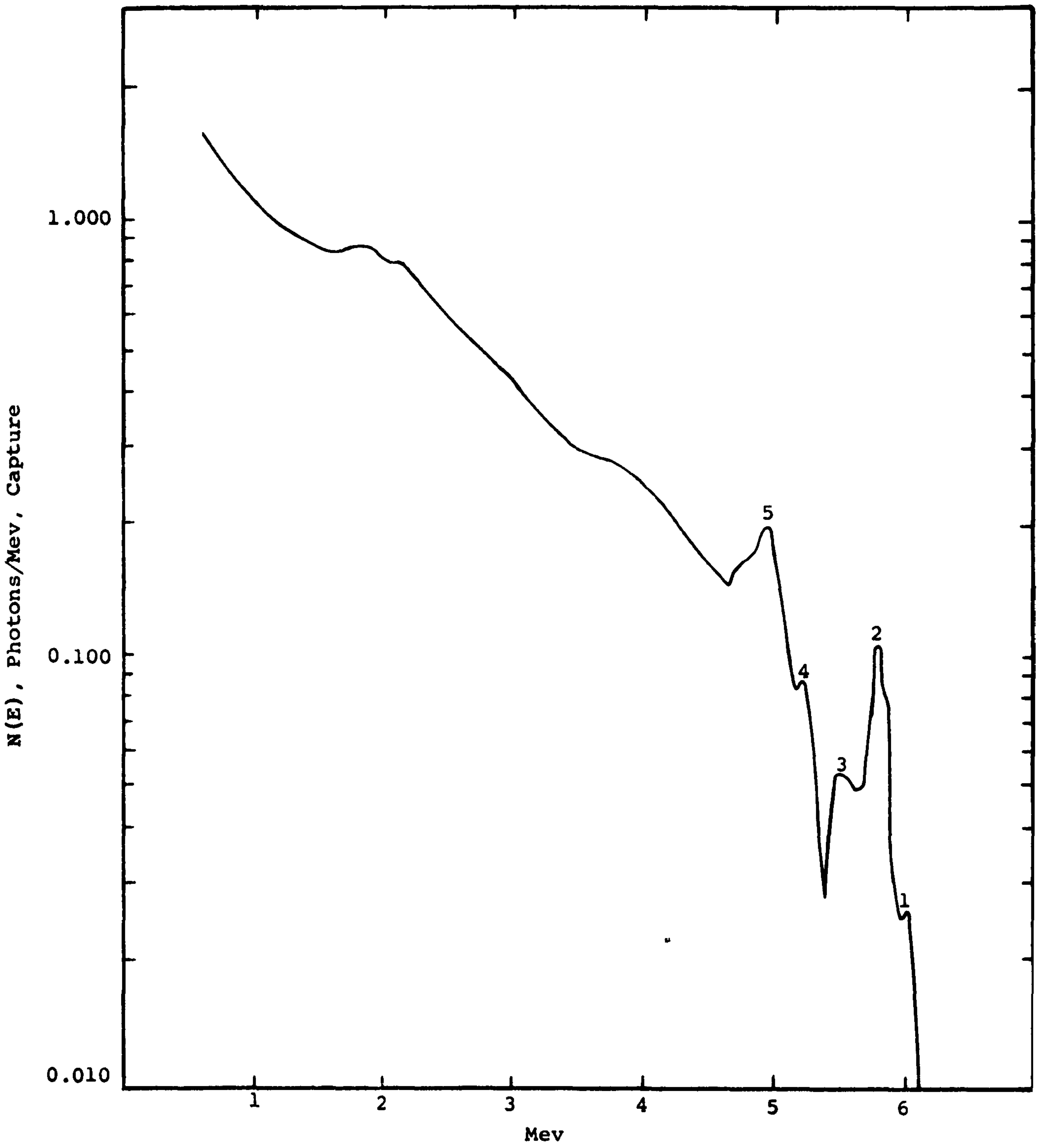

Figure 11. Capture Gamma Ray Spectrum of Re

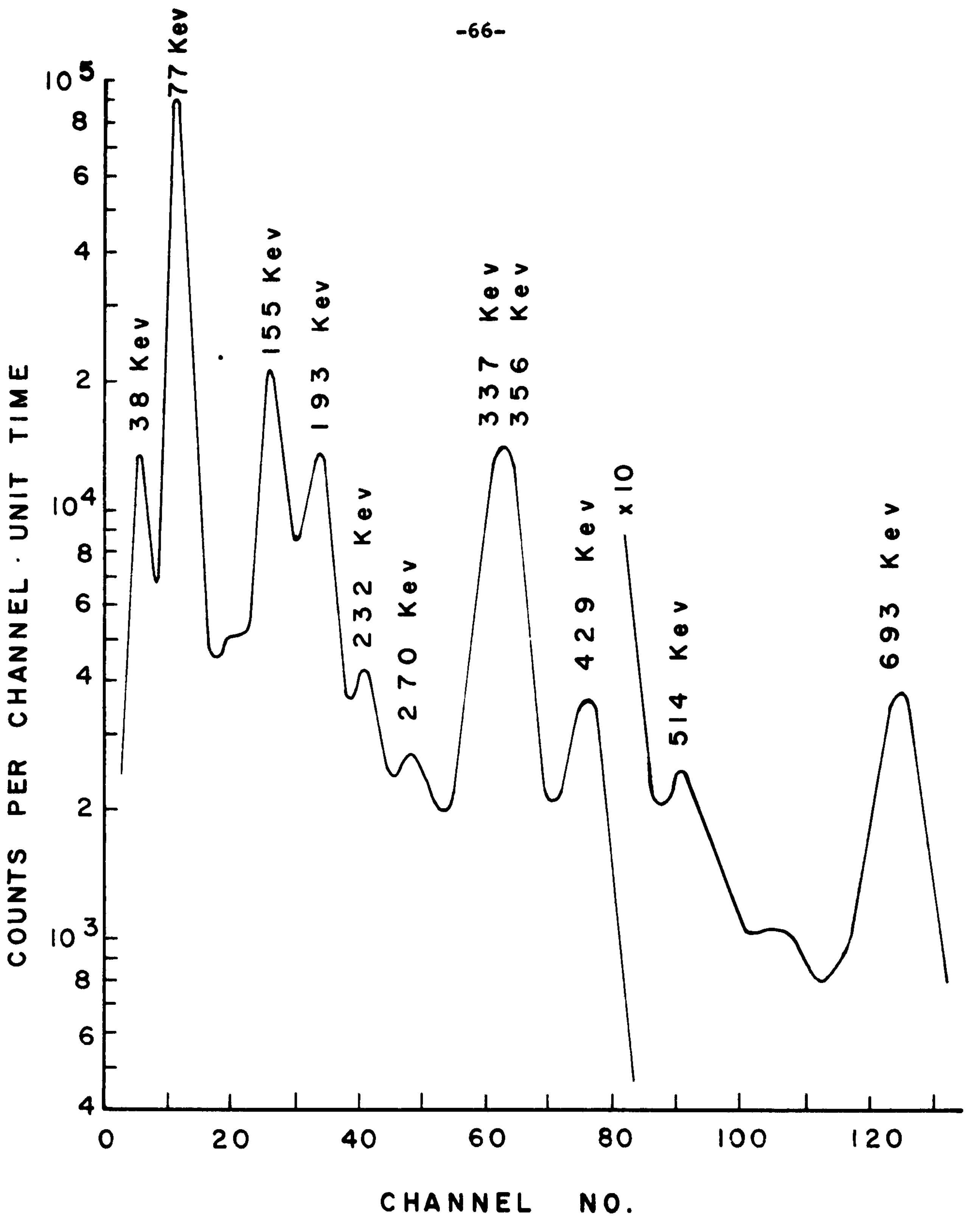

FIGURE 12. PULSE-HEIGHT SPECTRUM OF AU^{196} AND AU^{196m}

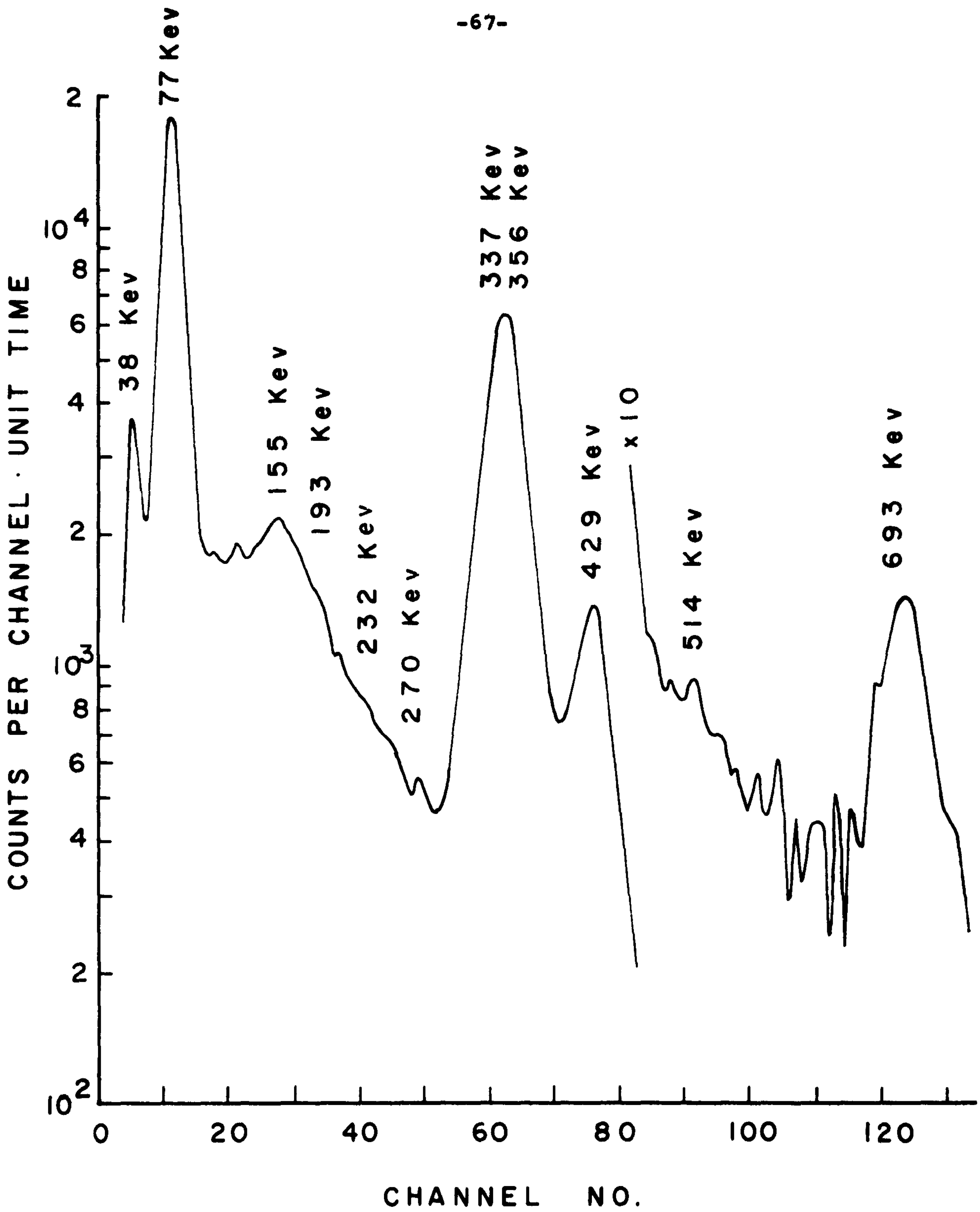

FIGURE 13. PULSE-HEIGHT SPECTRUM OF AU^{196}

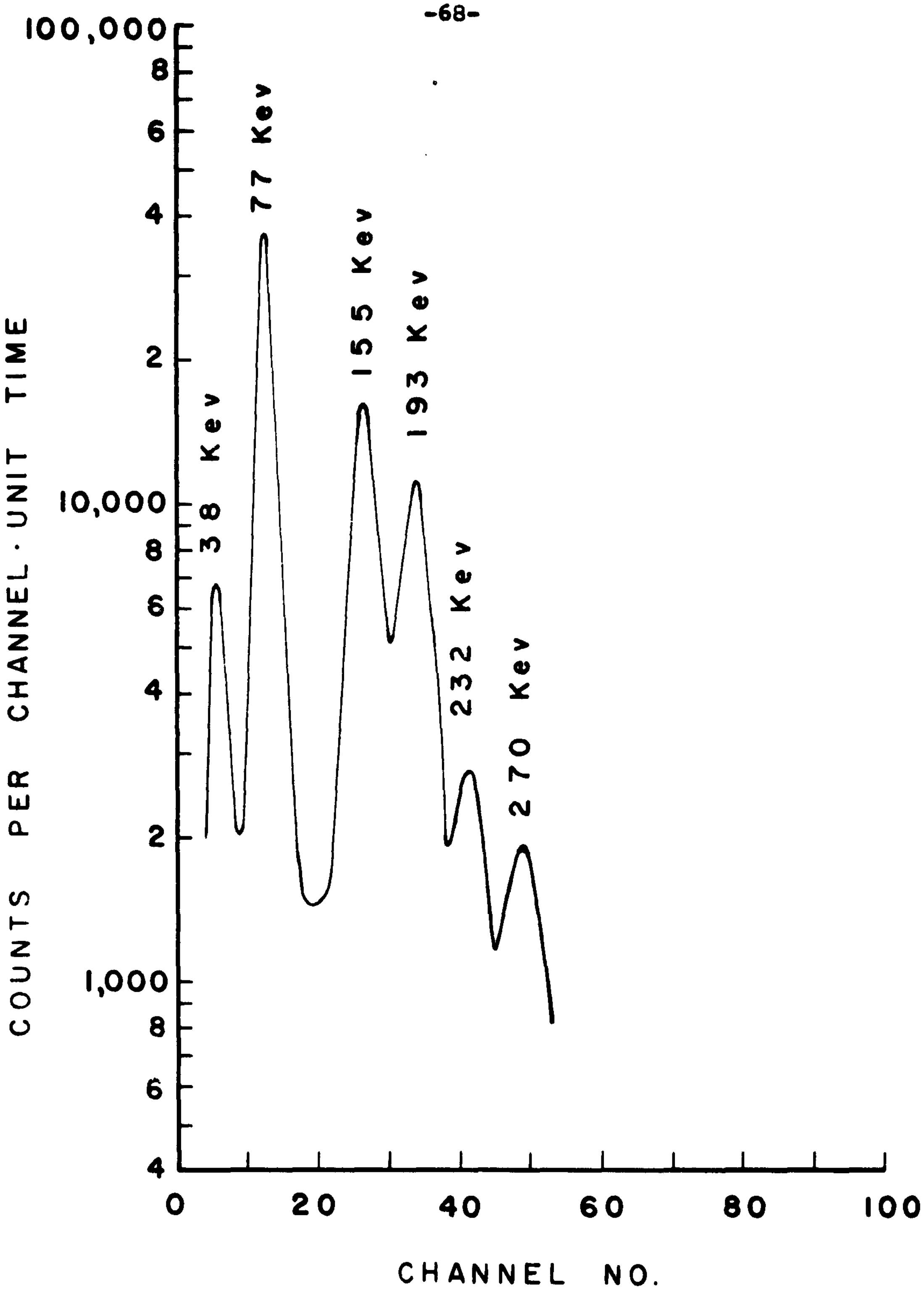

FIGURE 14. PULSE-HEIGHT SPECTRUM OF AU^{196m}

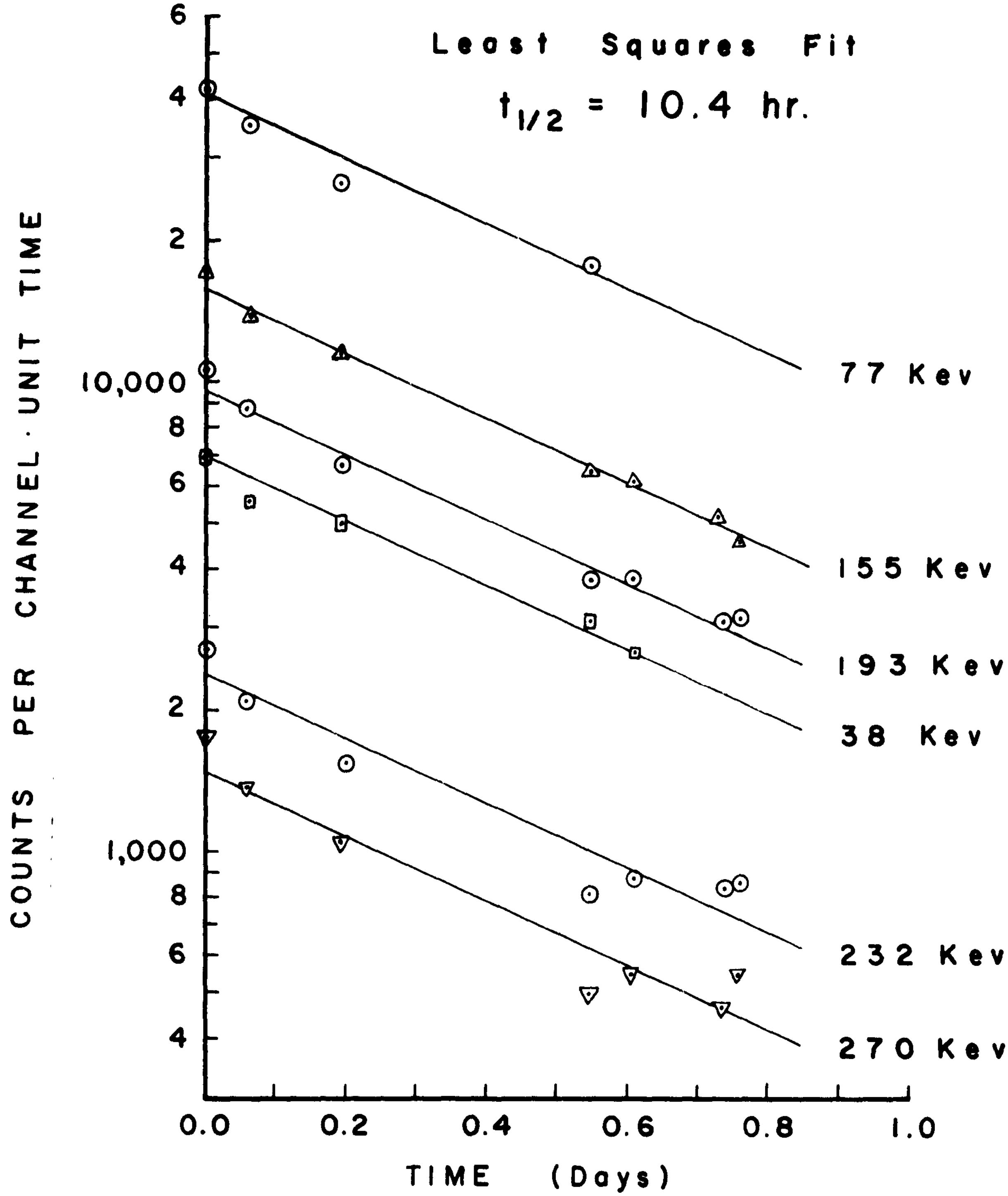

FIGURE 15. DECAY OF GAMMA RAYS FROM ISOMERIC TRANSITION OF AU^{196m} VS. TIME

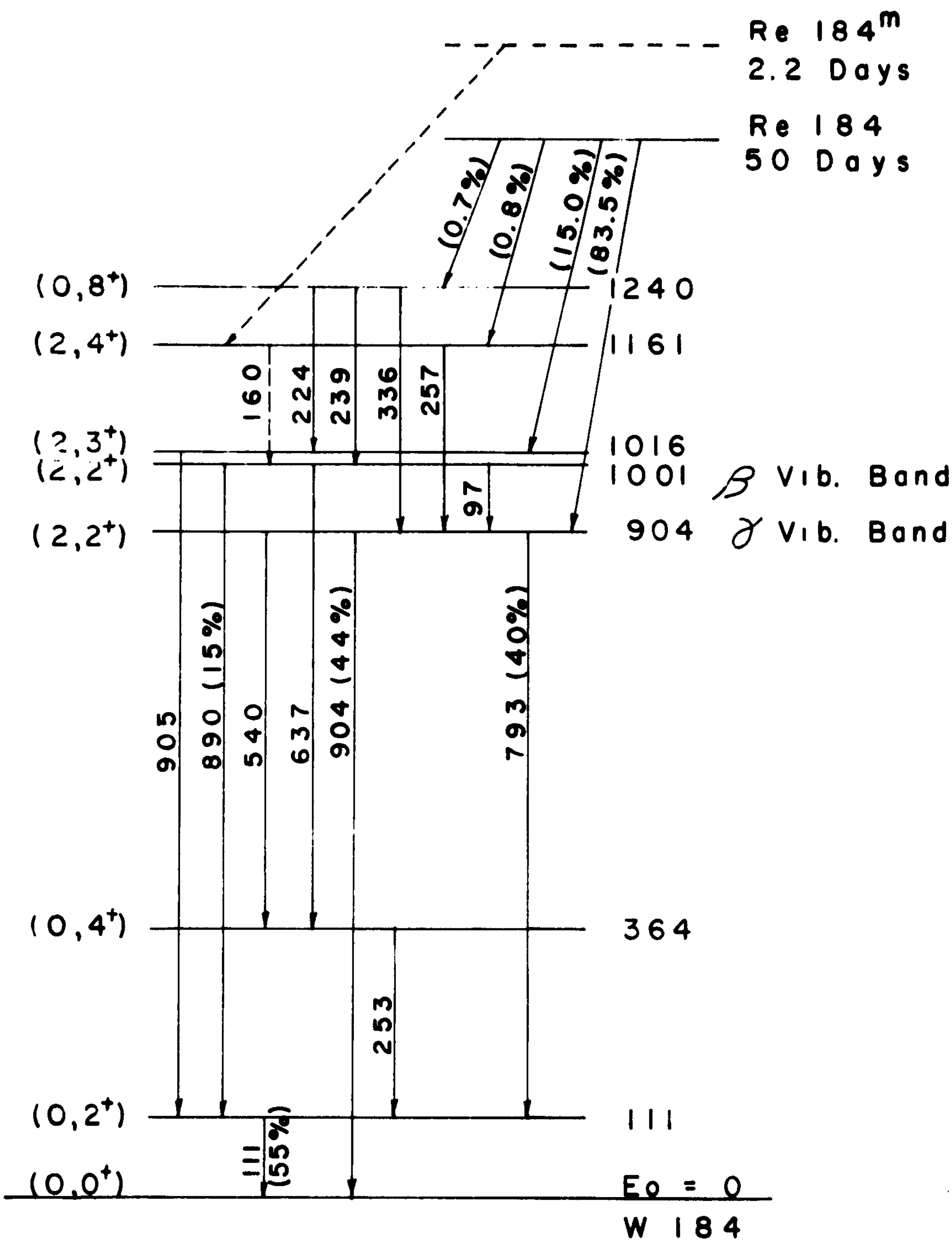

FIGURE 16 : DECAY SCHEME OF
Re 184 AND Re 184^m

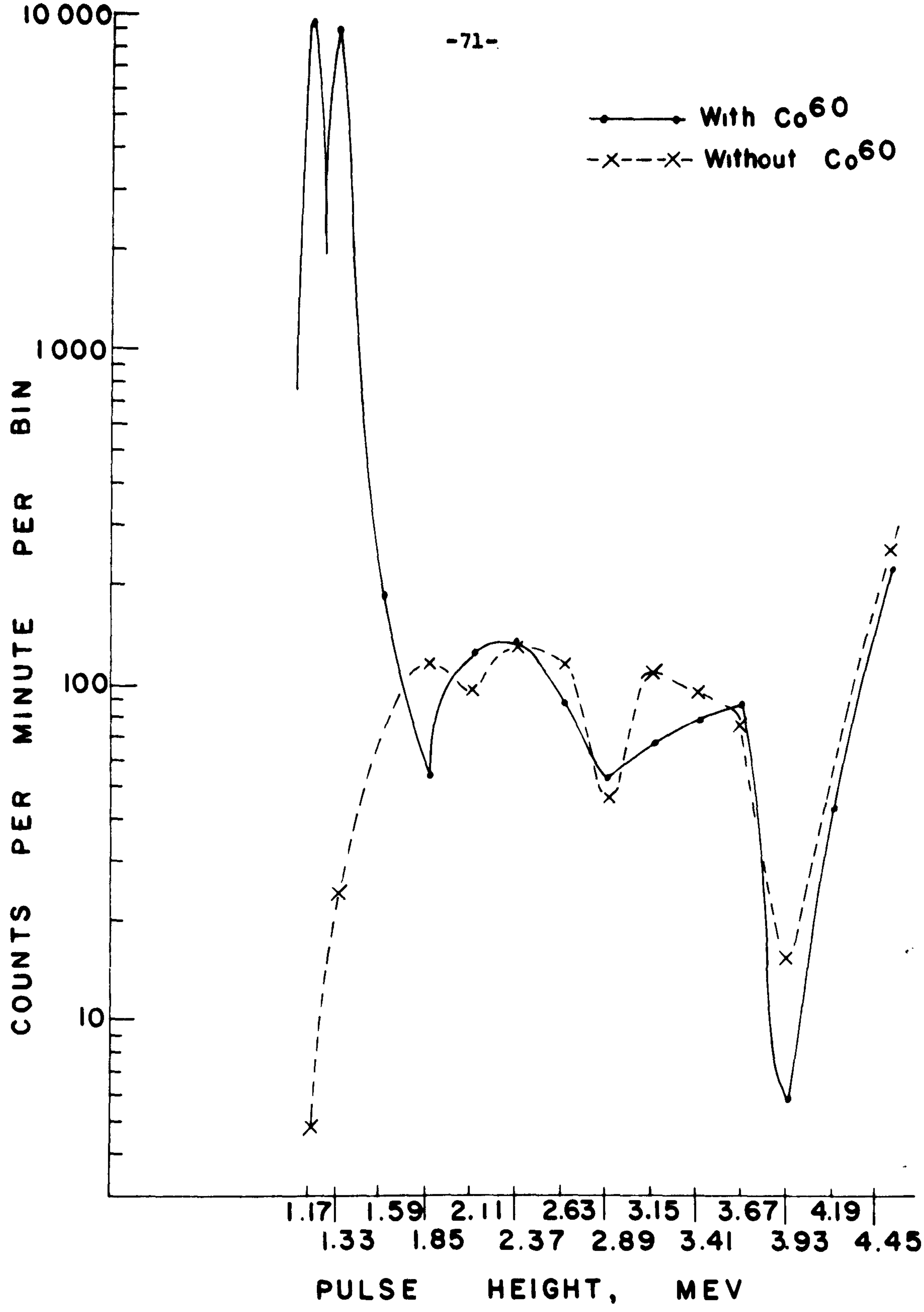

Separated Gamma-Ray Pulse-Height Distributions

Figure 17

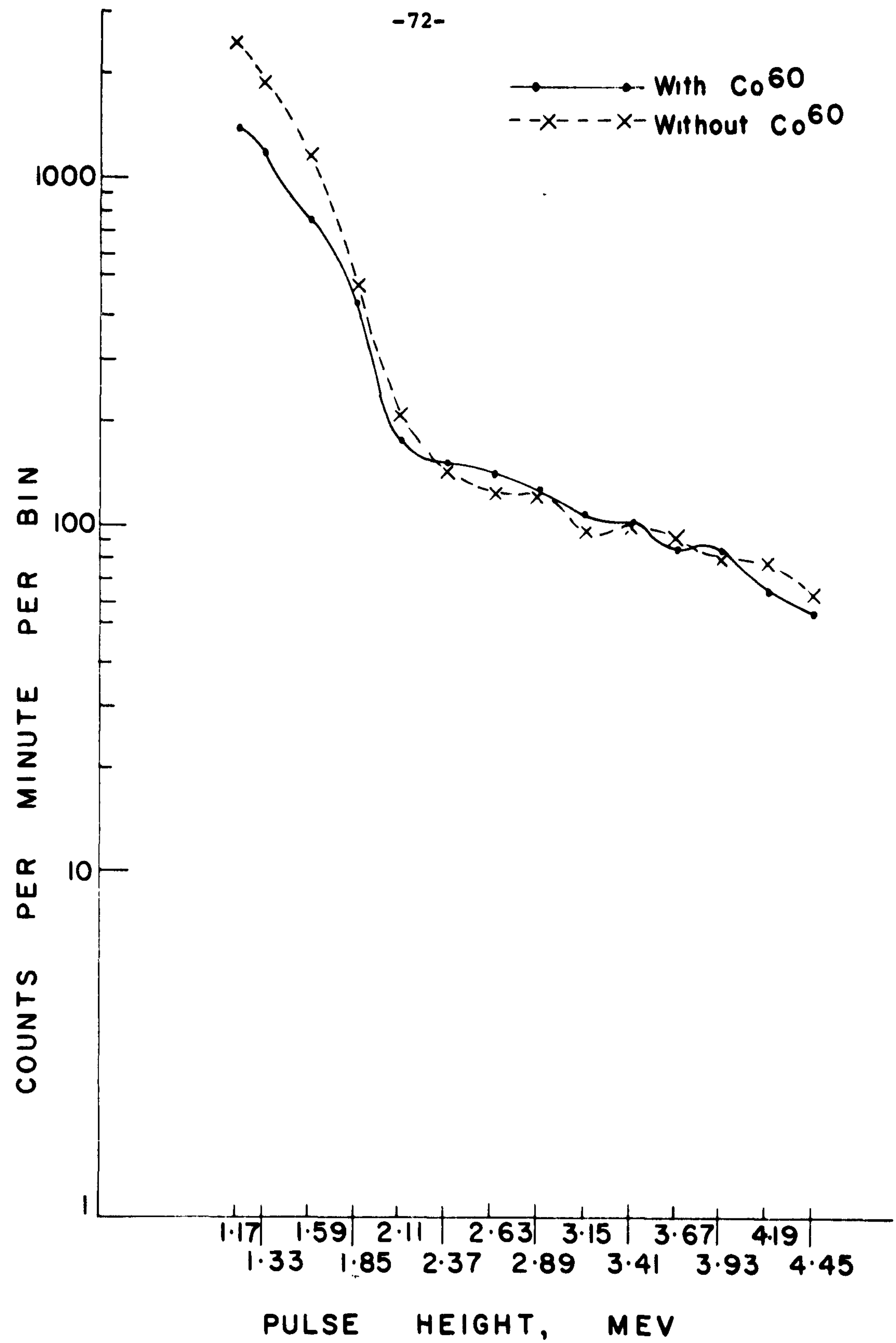

Separated Neutron Pulse-Height Distributions

Figure 18